
A CLASSIFYING TOPOS FOR THE SPECTRUM OF EQUIVALENCES

KENAN OGGAD

Université Paris-Saclay
e-mail address: kenan.oggad@universite-paris-saclay.fr

ABSTRACT. What makes two computational systems equivalent? Topos theory answers with classifying toposes: a system’s semantic content is encoded in the geometric theory it classifies, and two presentations are equivalent when their classifying toposes coincide. Process algebra answers with the linear time–branching time spectrum of van Glabbeek: a hierarchy of behavioral equivalences from trace equivalence to bisimilarity, each determined by which observations can distinguish processes. We show that these answers are aspects of a single structure, and develop the foundations of a topos-geometric theory of semantic equivalence in which behavioral abstraction is localization.

Each labeled transition system \mathcal{M} receives a geometric theory $\mathbb{T}_{\mathcal{M}}$ whose classifying topos $\mathcal{E}[\mathbb{T}_{\mathcal{M}}]$ determines its provable geometric sequents. We establish a strict hierarchy where mutual simulation is strictly coarser than bisimulation, which is strictly coarser than topos equivalence, and identify the boundary: diamond-only Hennessy–Milner logic characterizes the bisimulation-invariant fragment of geometric logic. This geometric analogue of van Benthem’s theorem is proved in full generality via bounded tree unraveling. Explicit Grothendieck topologies yield a strict chain $J_{\text{bisim}} \subsetneq J_{\text{sim}} \subsetneq J_{\text{trace}}$, constructive for trace and bisimulation; a constructive counterexample proves the naive existence-based observation-class approach provably inadequate for simulation, motivating Caramello’s quotient-theory duality as the natural alternative; an energy–topology framework extends this embedding to all 13 named equivalences of the spectrum.

Closing the named equivalences under lattice operations yields exactly 30 elements, including 17 unnamed hybrids absent from the classical spectrum because the energy-game framework computes but does not close. Lattice L_{30} is directly indecomposable; its Heyting implication $S \rightarrow F = \text{IF}$ identifies impossible futures as the algebraic mediator of the simulation–failures divide. A Geometric Closure Theorem computes presheaf Heyting implications by testing at a single free extension. All three levels of the hierarchy, the L_{30} bi-Heyting structure, and the Geometric Closure Theorem are proved constructively, a result internal to the topos with no known process-algebraic proof. Viewed through the classifying topos, the spectrum is a finite sub-poset of an infinite coframe whose algebraic operations (meets, implications, subtractions) produce structure inaccessible from within process algebra. All constructions are formalized in Lean 4 with Mathlib.

1. INTRODUCTION

Topos theory and process algebra offer independent frameworks for when two computational systems should be considered equivalent: the former through classifying toposes and their lattices of subtoposes, the latter through behavioral observation hierarchies culminating in van Glabbeek’s spectrum. We show that these perspectives fit within a single structure—the spectrum embeds as a finite sub-poset of the coframe of subtoposes of the classifying topos—by constructing explicit Grothendieck topologies for trace and bisimulation equivalence on

a classifying topos of labeled transition systems and completing the strict chain $J_{\text{bisim}} \subsetneq J_{\text{sim}} \subsetneq J_{\text{trace}}$ via Caramello’s quotient-theory duality. Simulation requires this indirect route: trace and bisimulation coverages operate at the sieve level (0-truncated), but simulation requires only homomorphism existence ((−1)-truncated), a truncation-level mismatch that *provably prevents* naive existence-based observation-class extensions (Theorem 6.5).

An energy–topology framework extends this three-point embedding to all 13 named process equivalences of the van Glabbeek spectrum. Assignment $E \mapsto J_E$ is antitone; the induced coframe map is injective for $|L| \geq 2$ and reveals algebraic structure invisible to the original spectrum: the coframe meet of two named-equivalence subtoposes can produce elements with no process-algebraic name (Theorem 6.10). It connects Bisping’s energy-game hierarchy to Lawvere–Tierney topologies through a chain: energy budget \rightarrow observation class \rightarrow covering predicate \rightarrow Grothendieck topology \rightarrow subtopos, an instance of Caramello’s bridge technique [12]:

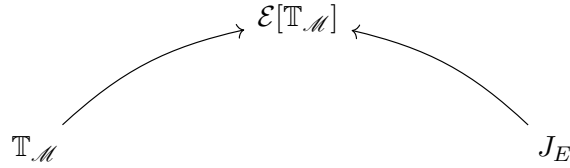


Figure 1: The geometric theory $\mathbb{T}_{\mathcal{M}}$ classifies the LTS structure; each topology J_E localizes the classifying topos to the subtopos enforcing the corresponding equivalence. The middle topology J_{sim} is the first requiring Caramello’s quotient-theory machinery; the 10 intermediate equivalences of the Energy–LT Bridge depend on it as well (§6.2).

Our topos-theoretic framework does not merely rederive known process-algebraic results; it provides the algebraic context in which new questions become natural. Process algebra is Turing-complete; that these results *could* in principle be computed without topos theory is a triviality. What topos theory provides is the conceptual lens: the coframe distributive law, the Heyting implication $S \rightarrow F = \text{IF}$, and the 17 unnamed spectrum elements are consequences of asking “what is the lattice of all behavioral abstractions?”, a question that requires the subtopos coframe to formulate. Each subtopos of the classifying topos corresponds to a choice of which geometric properties to retain; the spectrum structure emerges from the coframe of all such choices. This contrasts with the closest sheaf-theoretic precedent: Eberhart, Hirschowitz, and Seiller [16] construct a single Grothendieck topology enforcing bisimulation on interaction trees for the π -calculus; our approach fixes the site (f.p.LTS_L) and varies the topology across the *entire* spectrum, producing a lattice of subtoposes rather than a single quotient.

Two features of the bridge are irreducibly topos-theoretic. Its subtopos lattice carries coframe structure: meets distribute over joins, providing the spectrum with semantic lattice operations it does not intrinsically possess; while one can close the spectrum under meets and joins in a product frame, the coframe law is an invariant of the classifying topos, not of the energy-game representation (indeed, the lattice closure itself depends on the coordinatization: Remark 5.3). Furthermore, the coframe meet of two named equivalences can produce elements not generated by any single energy-game: the 17 unnamed elements in the lattice closure have concrete energy 6-tuples yet correspond to no named process equivalence.

Our construction proceeds through three stages. First, each system \mathcal{M} receives a geometric theory $\mathbb{T}_{\mathcal{M}}$ whose classifying topos $\mathcal{E}[\mathbb{T}_{\mathcal{M}}]$ determines its provable geometric sequents; explicit separating pairs—the fork \mathcal{F} versus the path \mathcal{P} , the hub-spokes \mathcal{H} versus the two-cycle \mathcal{C} —establish a strict three-level hierarchy from mutual simulation through bisimulation to topos equivalence (Theorems 3.10–3.12; §3). Hub-spokes’ 5-element Lindenbaum algebra and 8 Grothendieck topologies give a concrete instance of the full spectrum stratification (§3). Second, a geometric van Benthem theorem identifies the bisimulation-invariant fragment of geometric logic with diamond-only Hennessy–Milner logic: the forward direction is proved constructively (Theorem 4.2), and the converse is established via bounded tree unraveling (Theorem 4.12), with independent confirmation at depths ≤ 2 (Theorems 4.7–4.10; §4). Third, energy budgets determine Grothendieck topologies: J_{bisim} and J_{trace} receive constructive covering predicates, a constructive counterexample shows the observation-class approach provably fails for simulation (Theorem 6.5), and J_{sim} completes the chain via Caramello’s duality (Corollary 6.6). Energy–LT extends this to all 13 named equivalences (Theorem 6.10), and lattice closure yields the 30-element spectrum lattice L_{30} , whose bi-Heyting structure is detailed in §5–§6.2. At the presheaf level, the Geometric Closure Theorem reduces Heyting implication to testing at a single canonical free extension (Theorem 6.16; §6.5), making the coframe operations concretely computable.

2. GEOMETRIC THEORIES AND CLASSIFYING TOPOSES

Geometric logic is the fragment of first-order logic closed under \wedge , \vee (including infinitary), \exists , and \top ; all theories in this paper are finitary. This fragment is natural for toposes because geometric morphisms preserve exactly these connectives [25].

A *geometric theory* \mathbb{T} over a language \mathcal{L} consists of axioms in the form of *geometric sequents* $\phi \vdash_{\vec{x}} \psi$, where ϕ and ψ are geometric formulas. A *model* of \mathbb{T} in a topos \mathcal{E} interprets the sorts, function symbols, and relation symbols of \mathcal{L} as objects and morphisms in \mathcal{E} , satisfying all axioms of \mathbb{T} .

The *classifying topos* $\mathcal{E}[\mathbb{T}]$ is the universal topos representing \mathbb{T} : for any Grothendieck topos \mathcal{E} , there is an equivalence between geometric morphisms $\mathcal{E} \rightarrow \mathcal{E}[\mathbb{T}]$ and models of \mathbb{T} in \mathcal{E} , so that the study of models in any topos reduces to the study of geometric morphisms. It is constructed as the sheaf topos on the *syntactic category* $\mathbf{C}_{\mathbb{T}}$ —whose objects are formulas-in-context and whose morphisms are provably functional relations—with the syntactic topology generated by the axioms of \mathbb{T} [29]. Two geometric theories over the same language have equivalent classifying toposes if and only if they prove the same geometric sequents: the generic model in $\mathcal{E}[\mathbb{T}]$ validates exactly the geometric consequences of \mathbb{T} [25, D1.4.3]. This is our invariant: provable sequents distinguish classifying toposes.

A *bi-interpretation* between geometric theories \mathbb{T} and \mathbb{T}' consists of an interpretation $I: \mathbb{T} \rightarrow \mathbb{T}'$ and an interpretation $J: \mathbb{T}' \rightarrow \mathbb{T}$ such that the round-trip composites JI and IJ are definably isomorphic to the respective identities. If $\mathbb{T} \rightleftarrows \mathbb{T}'$, the Comparison Lemma [25, Theorem C2.2.3] implies $\mathcal{E}[\mathbb{T}] \simeq \mathcal{E}[\mathbb{T}']$. Its converse does not hold: bi-interpretation is strictly stronger than Morita equivalence [12]. In Section 3, we will specialize this theory-level notion to rooted transition systems, where it becomes a condition on simulations.

Definition 2.1 (Bisimulation-invariant sequent). A geometric sequent $\phi \vdash_{\vec{x}} \psi$ over a relational signature is *bisimulation-invariant* if for every relational bisimulation R between systems M and N (defined precisely in Definition 3.5): if $M \models \phi \vdash_{\vec{x}} \psi$ then $N \models \phi \vdash_{\vec{x}} \psi$.

3. ROOTED TRANSITION SYSTEMS AND THE THREE-LEVEL HIERARCHY

A *rooted transition system* \mathcal{M} consists of a set $S_{\mathcal{M}}$ of states, a transition relation on $S_{\mathcal{M}}$, and an initial state $\star_{\mathcal{M}} \in S_{\mathcal{M}}$. A *simulation* $f: \mathcal{M} \rightarrow \mathcal{N}$ is a function $f: S_{\mathcal{M}} \rightarrow S_{\mathcal{N}}$ that preserves transitions ($s \rightarrow s'$ in \mathcal{M} implies $f(s) \rightarrow f(s')$ in \mathcal{N}) and initial states ($f(\star_{\mathcal{M}}) = \star_{\mathcal{N}}$). Simulations compose and include identities, so rooted transition systems form a category.

To each rooted transition system \mathcal{M} we associate a geometric theory $\mathbb{T}_{\mathcal{M}}$ over the *rooted transition language* $\mathcal{L}_{\mathcal{M}}$ with sort S , constants c_s for each state $s \in S_{\mathcal{M}}$ (including a distinguished constant init for the initial state), and binary predicates Δ (transition), Γ (reachability), Θ (path equivalence). The theory $\mathbb{T}_{\mathcal{M}}$ consists of two components:

- (1) *Structural axioms* (6 sequents): $\Delta(x, y) \vdash \Gamma(x, y)$, $\top \vdash \Gamma(x, x)$, transitivity, Θ definition, Θ symmetry, and $\Theta \vdash \Gamma$.
- (2) *System-specific axioms*: for each transition $s \rightarrow t$ in \mathcal{M} , the existence axiom $\top \vdash \Delta(c_s, c_t)$; for each state s , the completeness axiom $\Delta(c_s, x) \vdash x = c_{t_1} \vee \cdots \vee x = c_{t_n}$ where $\{t_1, \dots, t_n\}$ is the set of successors of s (when s has no successors, the disjunction is empty, yielding $\Delta(c_s, x) \vdash \perp$); negative axioms $\Gamma(c_s, c_t) \vdash \perp$ for each non-reachable pair and $\Theta(c_s, c_t) \vdash \perp$ for each non-path-equivalent pair (pinning down all three predicates from above, not only from below); and the domain closure axiom $\top \vdash x = c_{s_1} \vee \cdots \vee x = c_{s_k}$ where $\{s_1, \dots, s_k\} = S_{\mathcal{M}}$.

These are all geometric sequents. The theory $\mathbb{T}_{\mathcal{M}}$ records the structural properties of \mathcal{M} expressible in geometric logic, including branching degree, local determinism, and confluence patterns. The classifying topos $\mathcal{E}[\mathbb{T}_{\mathcal{M}}]$ is the classifying topos of $\mathbb{T}_{\mathcal{M}}$. For finite-state systems, $\mathbb{T}_{\mathcal{M}}$ is finite; the construction is effective.

Lemma 3.1 (Soundness and Completeness). *Geometric provability from $\mathbb{T}_{\mathcal{M}}$ coincides with semantic validity.*

- (1) Soundness. *If a geometric sequent s is provable from a geometric theory \mathbb{T} , then every model of \mathbb{T} satisfies s .*
- (2) Completeness. *A geometric sequent s is provable from $\mathbb{T}_{\mathcal{M}}$ if and only if the canonical model satisfies s .*

Proof. Soundness is by structural induction on the derivation: axioms hold by hypothesis, cut composes, and the geometric connectives (\wedge , \vee , \exists) preserve satisfaction. For completeness, the generic model in $\mathcal{E}[\mathbb{T}_{\mathcal{M}}]$ validates exactly the provable geometric sequents [12, Cor. 2.1.12]. The system-specific axioms determine any Set-model of $\mathbb{T}_{\mathcal{M}}$ up to isomorphism: domain closure forces every element to equal some c_s ; the existence and completeness axioms pin down Δ ; and the negative axioms pin down Γ and Θ . Since $\mathbb{T}_{\mathcal{M}}$ is coherent (all disjunctions are finite for finite-state systems), its classifying topos has enough Set-points by Deligne's theorem [25, D3.3.13]. Thus: the canonical model satisfies $s \Rightarrow$ every Set-model satisfies s (uniqueness) \Rightarrow the generic model satisfies s (enough points) $\Rightarrow s$ is provable. The converse is soundness applied to the canonical model. \square

The separation proofs in §§3.2–3.3 and §4.3 rely on four *semantic bridge lemmas* that characterize when the separating sequents hold: σ_{tot} holds iff every state has a successor, σ_{det} holds iff the transition relation is functional, σ_{conf} holds iff every pair of successors has a common successor, and σ_{loop} holds iff every state has a self-loop.

Remark 3.2 (Size of the theory). For a finite system with $|S_{\mathcal{M}}|$ states, $\mathbb{T}_{\mathcal{M}}$ is finite: 6 structural axioms, at most $|S_{\mathcal{M}}|^2$ existence axioms, $|S_{\mathcal{M}}|$ completeness axioms, $O(|S_{\mathcal{M}}|^2)$ negative axioms for Γ and Θ , and one domain closure axiom, for $O(|S_{\mathcal{M}}|^2)$ sequents in total. For infinite systems the completeness and domain closure axioms may involve infinite disjunctions (geometric but no longer coherent); the classifying topos exists regardless [25, D1.4]. All witness systems in this paper are finite.

Definition 3.3 (Path equivalence). Two states $s, t \in S_{\mathcal{M}}$ are *path-equivalent*, written $s \sim t$, if they reach exactly the same states and are reached from exactly the same states: $s \sim t$ iff for all $u \in S_{\mathcal{M}}$, $s \rightarrow^* u \Leftrightarrow t \rightarrow^* u$ and $u \rightarrow^* s \Leftrightarrow u \rightarrow^* t$.

Path equivalence is an equivalence relation. The key property is that it is implied by mutual reachability.

Lemma 3.4 (Lifting Lemma). *In any rooted transition system \mathcal{M} :*

$$\boxed{s \rightarrow^* t \text{ and } t \rightarrow^* s \implies s \sim t}$$

Proof. Suppose $s \rightarrow^* t$ and $t \rightarrow^* s$. We must show that s and t reach exactly the same states and are reached from exactly the same states. If $s \rightarrow^* u$, then $t \rightarrow^* s \rightarrow^* u$, so $t \rightarrow^* u$. If $t \rightarrow^* u$, then $s \rightarrow^* t \rightarrow^* u$, so $s \rightarrow^* u$. If $u \rightarrow^* s$, then $u \rightarrow^* s \rightarrow^* t$, so $u \rightarrow^* t$. If $u \rightarrow^* t$, then $u \rightarrow^* t \rightarrow^* s$, so $u \rightarrow^* s$. Thus $s \sim t$. \square

Definition 3.5 (Relational bisimulation). A *relational bisimulation* between rooted transition systems \mathcal{M} and \mathcal{N} is a relation $R \subseteq S_{\mathcal{M}} \times S_{\mathcal{N}}$ satisfying the back-and-forth lifting property: if $(s, t) \in R$ and $s \rightarrow s'$ in \mathcal{M} , then there exists t' with $t \rightarrow t'$ in \mathcal{N} and $(s', t') \in R$ (*forth*); and if $(s, t) \in R$ and $t \rightarrow t'$ in \mathcal{N} , then there exists s' with $s \rightarrow s'$ in \mathcal{M} and $(s', t') \in R$ (*back*). The systems \mathcal{M} and \mathcal{N} are *bisimilar*, written $\mathcal{M} \approx \mathcal{N}$, if there exists a relational bisimulation R with $(\star_{\mathcal{M}}, \star_{\mathcal{N}}) \in R$.

We also introduce a stronger, functorial notion that connects to bi-interpretation.

Definition 3.6 (Functional bisimulation). A *functional bisimulation* between rooted transition systems \mathcal{M} and \mathcal{N} is a pair of simulations $f: \mathcal{M} \rightarrow \mathcal{N}$, $g: \mathcal{N} \rightarrow \mathcal{M}$ with $gf(s) \sim_{\mathcal{M}} s$ for all $s \in S_{\mathcal{M}}$ and $fg(t) \sim_{\mathcal{N}} t$ for all $t \in S_{\mathcal{N}}$.

In the coalgebraic literature, “functional bisimulation” sometimes denotes a single function whose graph is a relational bisimulation, i.e. a coalgebra homomorphism [36]. Our usage is distinct: we require a *pair* of simulations with round-trip path-equivalence coherence, capturing bi-interpretation rather than one-sided functional witnessing.

Every functional bisimulation implies relational bisimilarity. The converse does not hold: relational bisimilarity does not in general imply the existence of a functional bisimulation (see Remark 3.7). Throughout this paper, “bisimulation” refers to the relational notion of Park and Milner [33, 31] (Definition 3.5) unless explicitly qualified as “functional.”

Remark 3.7 (Functional vs. relational bisimulation). Functional bisimulation is strictly stronger than relational bisimulation, even for image-finite systems. A relational bisimulation can relate one state in \mathcal{M} to many states in \mathcal{N} without requiring any functional coherence. For example, a system with a single self-looping state is relationally bisimilar to any total system (every state has a successor) via the total relation, since the back-and-forth conditions are trivially met when one side can always respond with its self-loop. However, no functional bisimulation need exist between such systems if their path-equivalence quotients differ.

The *self-loop system* \mathcal{L} has a single state a with transition $a \rightarrow a$ and initial state a . The *two-cycle* \mathcal{C} has states $\{x, y\}$ with transitions $x \rightarrow y$, $y \rightarrow x$ and initial state x (defined in full in §3.3).

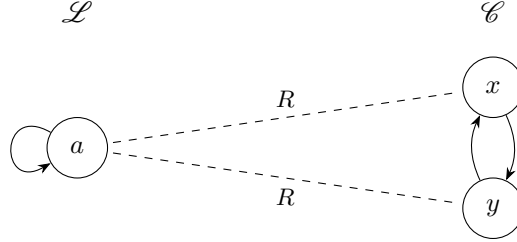


Figure 2: The self-loop \mathcal{L} and two-cycle \mathcal{C} . The dashed lines show the relational bisimulation $R = \{(a, x), (a, y)\}$. No simulation $\mathcal{L} \rightarrow \mathcal{C}$ exists: \mathcal{C} has no self-loops.

Proposition 3.8 (Functional vs. relational separation). *Functional bisimulation is strictly stronger than relational bisimulation. The systems \mathcal{L} and \mathcal{C} are relationally bisimilar (via $R = \{(a, x), (a, y)\}$) but not functionally bisimilar.*

Proof. Relational bisimulation. The relation $R = \{(a, x), (a, y)\}$ satisfies back-and-forth. At (a, x) : the transition $a \rightarrow a$ in \mathcal{L} is matched by $x \rightarrow y$ in \mathcal{C} with $(a, y) \in R$. At (a, y) : the transition $a \rightarrow a$ is matched by $y \rightarrow x$ with $(a, x) \in R$. Back conditions are symmetric.

No functional bisimulation. A functional bisimulation requires a simulation $f: \mathcal{L} \rightarrow \mathcal{C}$. The self-loop $a \rightarrow a$ must map to $f(a) \rightarrow f(a)$ in \mathcal{C} . But \mathcal{C} has no self-loops: x has unique successor $y \neq x$, and y has unique successor $x \neq y$. No simulation $\mathcal{L} \rightarrow \mathcal{C}$ exists, hence no functional bisimulation. \square

This is a refinement of the three-level hierarchy: together with the First and Second Separation theorems below, it yields four strict levels:

mutual simulation \supseteq relational bisimulation \supseteq functional bisimulation \supseteq topos equivalence.

The main narrative treats “bisimulation” as the relational notion (per the convention above), giving three principal levels; the functional–relational distinction is secondary.

3.1. Bi-interpretation of Systems. A *bi-interpretation of rooted transition systems* \mathcal{M} and \mathcal{N} , written $\mathcal{M} \rightleftarrows \mathcal{N}$, is a pair of simulations $f: \mathcal{M} \rightarrow \mathcal{N}$, $g: \mathcal{N} \rightarrow \mathcal{M}$ satisfying the weaker coherence condition that $gf(s)$ and s are *mutually reachable* ($gf(s) \rightarrow^* s$ and $s \rightarrow^* gf(s)$) for all $s \in S_{\mathcal{M}}$, and $fg(t)$ and t are mutually reachable for all $t \in S_{\mathcal{N}}$.

Despite the shared name, a bi-interpretation of systems does *not* induce a bi-interpretation of the associated geometric theories. A simulation $f: \mathcal{M} \rightarrow \mathcal{N}$ preserves all geometric sequents in the bisimulation-invariant fragment (the tree-shaped, equality-free formulas corresponding to *HML*), but need not preserve arbitrary geometric sequents of $\mathbb{T}_{\mathcal{M}}$; for instance, f can map a deterministic system into a non-deterministic one, losing the sequent σ_{det} . The gap between system-level bi-interpretation and theory-level bi-interpretation is exactly the content of the Second Separation (Theorem 3.12): bisimilar (hence mutually bi-interpretable, by Theorem 3.9) systems can have non-equivalent classifying toposes.

Theorem 3.9 (Functional Bisimulation–Bi-Interpretation Correspondence). *For all rooted transition systems \mathcal{M} and \mathcal{N} , there exists a functional bisimulation between \mathcal{M} and \mathcal{N} if and only if there exists a bi-interpretation between them:*

$$\boxed{\mathcal{M} \text{ and } \mathcal{N} \text{ are functionally bisimilar} \iff \mathcal{M} \rightleftarrows \mathcal{N}}$$

Proof. Forward, path equivalence implies mutual reachability, since if $s \sim t$ then in particular $s \rightarrow^* t$ and $t \rightarrow^* s$ (take $u = t$ and $u = s$ respectively in the definition of path equivalence; more precisely, $s \rightarrow^* s$ holds trivially, and $s \sim t$ gives $t \rightarrow^* s$, and symmetrically $s \rightarrow^* t$). Therefore any functional bisimulation is a bi-interpretation.

Conversely, the Lifting Lemma applies. Suppose $(f, g): \mathcal{M} \rightleftarrows \mathcal{N}$ is a bi-interpretation, so that $gf(s) \rightarrow^* s$ and $s \rightarrow^* gf(s)$ for all $s \in S_{\mathcal{M}}$, and $fg(t) \rightarrow^* t$ and $t \rightarrow^* fg(t)$ for all $t \in S_{\mathcal{N}}$. By Lemma 3.4, mutual reachability implies path equivalence: $gf(s) \sim_{\mathcal{M}} s$ for all s and $fg(t) \sim_{\mathcal{N}} t$ for all t . Thus (f, g) is a functional bisimulation. \square

With the framework in place, we establish the strict three-level hierarchy by exhibiting witnesses for each separation and proving a bridge theorem relating the two finer levels.

3.2. First Separation: Mutual Simulation \supseteq Bisimulation. The *fork* \mathcal{F} has states $\{a, b, c\}$, transitions $a \rightarrow b$, $a \rightarrow c$, and $b \rightarrow b$, and initial state a . The initial state a branches: one branch leads to a *halting* state c (no outgoing transitions), and the other to a self-looping state b . The *path* \mathcal{P} has states $\{x, y\}$, transitions $x \rightarrow y$ and $y \rightarrow y$, and initial state x . It is a single step followed by a self-loop.

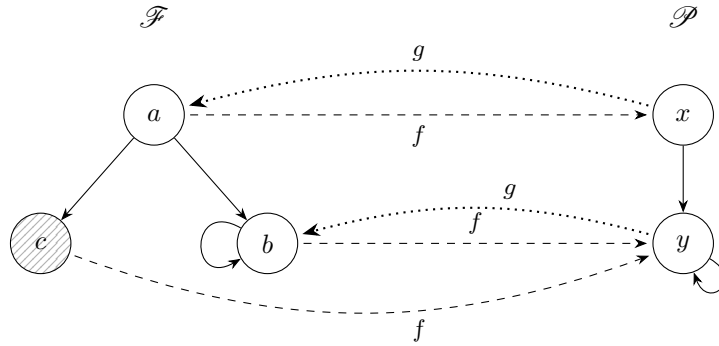


Figure 3: The fork \mathcal{F} and path \mathcal{P} with mutual simulations. Dashed arrows: $f(a) = x$, $f(b) = f(c) = y$. Dotted arrows: $g(x) = a$, $g(y) = b$. The halting state c (hatched) has no preimage under g .

Theorem 3.10 (First Separation). *The systems \mathcal{F} and \mathcal{P} mutually simulate. They are not bisimilar, and their classifying toposes are not equivalent:*

$$\boxed{\text{Hom}(\mathcal{F}, \mathcal{P}) \neq \emptyset, \text{Hom}(\mathcal{P}, \mathcal{F}) \neq \emptyset, \mathcal{F} \not\approx \mathcal{P}, \mathcal{E}[\mathbb{T}_{\mathcal{F}}] \not\approx \mathcal{E}[\mathbb{T}_{\mathcal{P}}]}$$

Proof. Mutual simulation. The simulation $f: \mathcal{F} \rightarrow \mathcal{P}$ is defined by $f(a) = x$, $f(b) = y$, $f(c) = y$. This preserves transitions: $a \rightarrow b$ maps to $x \rightarrow y$, $a \rightarrow c$ maps to $x \rightarrow y$, and $b \rightarrow b$ maps to $y \rightarrow y$. The halting state c has no outgoing transitions, so there is nothing to verify. It preserves the initial state: $f(a) = x$. The simulation $g: \mathcal{P} \rightarrow \mathcal{F}$ is defined by

$g(x) = a$, $g(y) = b$. This preserves transitions: $x \rightarrow y$ maps to $a \rightarrow b$, and $y \rightarrow y$ maps to $b \rightarrow b$. It preserves the initial state: $g(x) = a$.

Non-bisimilarity. Suppose for contradiction that R is a relational bisimulation with $(a, x) \in R$. The forth condition applied to the transition $a \rightarrow c$ in \mathcal{F} yields a state t' with $x \rightarrow t'$ in \mathcal{P} and $(c, t') \in R$. Since x has unique successor y , we have $t' = y$ and thus $(c, y) \in R$. Now apply the back condition at (c, y) : the transition $y \rightarrow y$ in \mathcal{P} requires a state s' with $c \rightarrow s'$ in \mathcal{F} and $(s', y) \in R$. But c has no outgoing transitions; it is a halting state. This is a contradiction.

Topos separation. The *totality sequent* $\sigma_{\text{tot}} := \top \vdash_x \exists y. \Delta(x, y)$ asserts that every state has a successor. This sequent is provable in $\mathbb{T}_{\mathcal{P}}$: state x has successor y , and state y has successor y . It is not provable in $\mathbb{T}_{\mathcal{F}}$: state c has no successor. Since σ_{tot} is a geometric sequent provable in $\mathbb{T}_{\mathcal{P}}$ but not in $\mathbb{T}_{\mathcal{F}}$, the two theories have different deductive closures. Provability of geometric sequents is invariant under equivalence of classifying toposes—it is detected by the generic model’s internal logic [25, D1.4.3]—so $\mathcal{E}[\mathbb{T}_{\mathcal{F}}] \not\equiv \mathcal{E}[\mathbb{T}_{\mathcal{P}}]$. \square

Remark 3.11 (Halting intuition). The First Separation has a natural computational interpretation. The fork \mathcal{F} can halt (by reaching state c), while the path \mathcal{P} cannot. Yet they mutually simulate: every simulation from \mathcal{P} into \mathcal{F} maps to the non-halting branch, and the simulation from \mathcal{F} to \mathcal{P} collapses the halting branch. Bisimulation, however, requires the back condition to hold at every related pair, and no state in \mathcal{P} can match the halting behavior of c .

3.3. Second Separation: Bisimulation \supseteq Topos Equivalence. The *hub-spokes system* \mathcal{H} has states $\{a, b, c\}$, transitions $a \rightarrow b$, $a \rightarrow c$, $b \rightarrow a$, $c \rightarrow a$, and initial state a . The hub a connects to two spokes b and c , each of which connects back to the hub. The *two-cycle* \mathcal{C} has states $\{x, y\}$, transitions $x \rightarrow y$, $y \rightarrow x$, and initial state x . It is a simple alternating cycle.

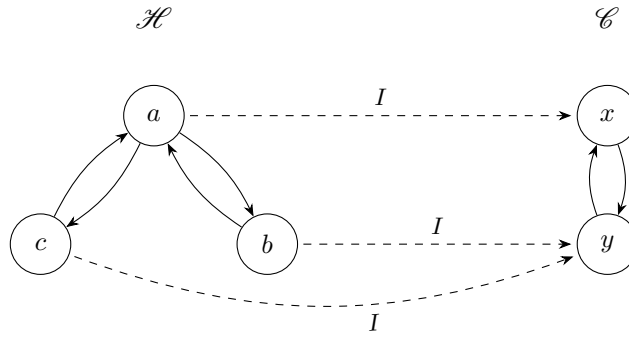


Figure 4: The hub-spokes \mathcal{H} and two-cycle \mathcal{C} . Dashed arrows show the simulation $I: \mathcal{H} \rightarrow \mathcal{C}$ with $I(a) = x$, $I(b) = I(c) = y$; the reverse simulation is $K(x) = a$, $K(y) = b$. Non-injectivity $I(b) = I(c)$ collapses the branching that σ_{det} detects.

Theorem 3.12 (Second Separation). *The systems \mathcal{H} and \mathcal{C} are bisimilar, yet their classifying toposes are not equivalent:*

$$\boxed{\mathcal{H} \approx \mathcal{C} \quad \text{yet} \quad \mathcal{E}[\mathbb{T}_{\mathcal{H}}] \not\equiv \mathcal{E}[\mathbb{T}_{\mathcal{C}}]}$$

Proof. Functional bisimulation. Define $I: \mathcal{H} \rightarrow \mathcal{C}$ by $I(a) = x$, $I(b) = y$, $I(c) = y$. This preserves transitions: $a \rightarrow b$ maps to $x \rightarrow y$, $a \rightarrow c$ maps to $x \rightarrow y$, $b \rightarrow a$ maps to $y \rightarrow x$, $c \rightarrow a$ maps to $y \rightarrow x$. Define $K: \mathcal{C} \rightarrow \mathcal{H}$ by $K(x) = a$, $K(y) = b$. This preserves transitions: $x \rightarrow y$ maps to $a \rightarrow b$, $y \rightarrow x$ maps to $b \rightarrow a$.

Coherence. The round-trips on \mathcal{H} are: $KI(a) = a$, $KI(b) = b$, and $KI(c) = b$. The first two are identities. For the third, $b \sim_{\mathcal{H}} c$ since $b \rightarrow a \rightarrow c$ and $c \rightarrow a \rightarrow b$ witness mutual reachability (Lemma 3.4). The round-trips on \mathcal{C} are: $IK(x) = x$ and $IK(y) = y$, both identities. Thus (I, K) is a functional bisimulation.

Relational bisimilarity. The relation $R = \{(a, x), (b, y), (c, y)\}$ is a relational bisimulation directly: at (a, x) , the transitions $a \rightarrow b$ and $a \rightarrow c$ are matched by $x \rightarrow y$ with $(b, y), (c, y) \in R$; at (b, y) , $b \rightarrow a$ is matched by $y \rightarrow x$ with $(a, x) \in R$; at (c, y) , $c \rightarrow a$ is matched by $y \rightarrow x$ with $(a, x) \in R$; back conditions are symmetric. Hence $\mathcal{H} \approx \mathcal{C}$.

Topos separation. The determinism sequent $\sigma_{\text{det}} := \Delta(x, y) \wedge \Delta(x, z) \vdash y = z$ is provable in $\mathbb{T}_{\mathcal{C}}$: state x has exactly one successor y , and state y has exactly one successor x . The sequent is not provable in $\mathbb{T}_{\mathcal{H}}$: state a has two distinct successors b and c with $b \neq c$. Since σ_{det} is a geometric sequent provable in $\mathbb{T}_{\mathcal{C}}$ but not in $\mathbb{T}_{\mathcal{H}}$, the two theories have different deductive closures. Provability of geometric sequents is invariant under equivalence of classifying toposes [25, D1.4.3], so $\mathcal{E}[\mathbb{T}_{\mathcal{H}}] \not\approx \mathcal{E}[\mathbb{T}_{\mathcal{C}}]$. \square

Remark 3.13 (Multiple witnesses). The Second Separation is not limited to the determinism sequent. In Section 4.3, two additional bisimilar pairs independently demonstrate non-equivalent classifying toposes: the diamond graph and confluence tree (separated by a weak confluence sequent), and the self-loop system and two-cycle (separated by a universal self-loop sequent).

Corollary 3.14 (Bi-interpretation does not imply topos equivalence). *System-level bi-interpretation does not imply topos equivalence: \mathcal{H} and \mathcal{C} satisfy $\mathcal{H} \rightleftarrows \mathcal{C}$ (bi-interpretation, by Theorem 3.9) and $\mathcal{H} \approx \mathcal{C}$ (relational bisimilarity), yet $\mathcal{E}[\mathbb{T}_{\mathcal{H}}] \not\approx \mathcal{E}[\mathbb{T}_{\mathcal{C}}]$.*

3.4. The Quotient Bridge. For a rooted transition system \mathcal{M} , the *path-equivalence quotient* \mathcal{M}/\sim has states $S_{\mathcal{M}}/\sim$, transitions $[s_1] \rightarrow [s_2]$ whenever some representatives have $s'_1 \rightarrow s'_2$ with $s'_1 \sim s_1$ and $s'_2 \sim s_2$, and initial state $[\star_{\mathcal{M}}]$. The quotient collapses path-equivalent states into single equivalence classes.

Theorem 3.15 (Quotient Bridge). *For all rooted transition systems \mathcal{M} and \mathcal{N} , if there exists a functional bisimulation between \mathcal{M} and \mathcal{N} , then their path-equivalence quotients have equivalent classifying toposes:*

$$\mathcal{M} \text{ and } \mathcal{N} \text{ are functionally bisimilar} \implies \mathcal{E}[\mathbb{T}_{\mathcal{M}/\sim}] \simeq \mathcal{E}[\mathbb{T}_{\mathcal{N}/\sim}]$$

Proof. Let (f, g) be a functional bisimulation between \mathcal{M} and \mathcal{N} . The argument has two steps: descent to quotients, then mutual inverse.

Well-definedness. We show f preserves path equivalence: if $s_1 \sim_{\mathcal{M}} s_2$, then $f(s_1) \sim_{\mathcal{N}} f(s_2)$. For forward reachability, suppose $f(s_1) \rightarrow^* v$ in \mathcal{N} ; we must show $f(s_2) \rightarrow^* v$. Since g is a simulation, $gf(s_1) \rightarrow^* g(v)$ in \mathcal{M} . The coherence condition $gf(s_1) \sim_{\mathcal{M}} s_1$ gives $s_1 \rightarrow^* g(v)$, and then $s_1 \sim_{\mathcal{M}} s_2$ gives $s_2 \rightarrow^* g(v)$. Since f is a simulation, $f(s_2) \rightarrow^* fg(v)$. The coherence condition $fg(v) \sim_{\mathcal{N}} v$ implies $fg(v) \rightarrow^* v$ (path equivalence implies mutual reachability), so $f(s_2) \rightarrow^* fg(v) \rightarrow^* v$. Backward reachability is symmetric. Thus f induces $\bar{f}: \mathcal{M}/\sim \rightarrow \mathcal{N}/\sim$ by $\bar{f}([s]) = [f(s)]$; similarly g induces \bar{g} .

Mutual inverse. The composite $\bar{g}\bar{f}([s]) = [gf(s)]$. The coherence condition $gf(s) \sim_{\mathcal{M}} s$ gives $[gf(s)] = [s]$, so $\bar{g}\bar{f} = \text{id}$. Symmetrically $\bar{f}\bar{g} = \text{id}$. Since f preserves both transitions and path equivalence, \bar{f} is a simulation of quotient systems; likewise \bar{g} . Thus \bar{f} and \bar{g} are mutually inverse simulations, giving $\mathcal{M}/\sim \cong \mathcal{N}/\sim$ as rooted transition systems. Isomorphic systems have identical geometric theories, hence equivalent classifying toposes. \square

By the Quotient Bridge, functional bisimulation preserves the classifying topos of the quotient, even though relational bisimulation need not preserve the classifying topos of the original system. The quotient collapses exactly the branching structure that the determinism sequent detects: in \mathcal{H}/\sim , the states b and c merge into $[b] = [c]$, making $\mathcal{H}/\sim \cong \mathcal{C}/\sim$.

Remark 3.16 (Functorial structure). The assignment $\mathcal{M} \mapsto \mathcal{E}[\mathbb{T}_{\mathcal{M}}]$ extends to a contravariant 2-functor $\mathcal{E}[-]: \mathbf{Mwy}^{\text{op}} \rightarrow \mathbf{BTop}$, where \mathbf{Mwy} is the 2-category of rooted transition systems, simulations, and path-equivalence homotopies, and \mathbf{BTop} is the 2-category of Grothendieck toposes, geometric morphisms, and geometric transformations. A simulation $f: \mathcal{M} \rightarrow \mathcal{N}$ induces a geometric morphism $f^*: \mathcal{E}[\mathbb{T}_{\mathcal{N}}] \rightarrow \mathcal{E}[\mathbb{T}_{\mathcal{M}}]$ by pulling back models along f ; a 2-cell $\alpha: f \Rightarrow g$ induces a geometric transformation $g^* \Rightarrow f^*$. In this language, the three-level hierarchy encodes three fiber conditions: mutual simulation means geometric morphisms exist both ways; functional bisimulation means they compose to equivalences on path-equivalence quotients (Theorem 3.15); topos equivalence means Morita equivalence of the geometric theories. Every such geometric morphism factors as hyperconnected (adding axioms) followed by localic (expanding the language); the Second Separation is purely hyperconnected, since the determinism sequent is an axiom over the same language. 2-functoriality follows from the standard fact that pullback of models along simulations preserves geometric morphism composition, and that path-equivalence homotopies lift to geometric transformations via the universal property of the syntactic category. In summary:

$$\mathcal{M} \xrightarrow{f} \mathcal{N} \quad \mapsto \quad \mathcal{E}[\mathbb{T}_{\mathcal{N}}] \xrightarrow{f^*} \mathcal{E}[\mathbb{T}_{\mathcal{M}}]$$

4. THE BISIMULATION-INVARIANT FRAGMENT

The hierarchy of Section 3 shows that geometric logic sees structure invisible to bisimulation, but does not explain *why*. This section identifies the boundary: the bisimulation-invariant fragment of geometric logic is exactly diamond-only Hennessy–Milner logic, and three syntactic mechanisms account for all the ways geometric logic crosses it.

4.1. Diamond-Only Hennessy–Milner Logic.

Definition 4.1 (HML). The *diamond-only Hennessy–Milner logic HML* is generated by:

$$\varphi ::= \top \mid \perp \mid \varphi_1 \wedge \varphi_2 \mid \varphi_1 \vee \varphi_2 \mid \diamond\varphi$$

The semantics at a state s in a rooted transition system \mathcal{M} are standard: $\mathcal{M}, s \models \top$ always; $\mathcal{M}, s \models \perp$ never; $\mathcal{M}, s \models \varphi_1 \wedge \varphi_2$ iff both conjuncts hold; $\mathcal{M}, s \models \varphi_1 \vee \varphi_2$ iff at least one disjunct holds; $\mathcal{M}, s \models \diamond\varphi$ iff there exists t with $s \rightarrow t$ and $\mathcal{M}, t \models \varphi$.

The *standard translation* embeds *HML* into the positive existential fragment of first-order logic over the rooted transition language:

$$\begin{aligned} \text{ST}_x(\top) &= \top & \text{ST}_x(\perp) &= \perp \\ \text{ST}_x(\varphi_1 \wedge \varphi_2) &= \text{ST}_x(\varphi_1) \wedge \text{ST}_x(\varphi_2) & \text{ST}_x(\varphi_1 \vee \varphi_2) &= \text{ST}_x(\varphi_1) \vee \text{ST}_x(\varphi_2) \\ \text{ST}_x(\diamond\varphi) &= \exists y. (\Delta(x, y) \wedge \text{ST}_y(\varphi)) \end{aligned}$$

The image of the standard translation has three distinctive properties. First, it is *equality-free*: no equality symbol appears. Second, it has *linear variables*: each existentially bound variable y appears in exactly one Δ -atom as target and in no other atom position. Third, it has *tree-shaped dependencies*: the variable dependency graph (where $x \rightarrow y$ means y is introduced in a \diamond under x) is a forest. In the terminology of database theory [42], the standard translation produces exactly the *acyclic conjunctive queries* over the binary relation Δ .

4.2. Forward Direction: HML Is Bisimulation-Invariant.

Theorem 4.2 (HML Bisimulation Invariance). *Let R be a relational bisimulation between rooted transition systems \mathcal{M} and \mathcal{N} , and let $(s, t) \in R$. For any HML formula φ :*

$$\boxed{\mathcal{M}, s \models \varphi \iff \mathcal{N}, t \models \varphi}$$

Proof. We prove both directions simultaneously by structural induction on φ . The case $\varphi = \top$ is immediate since \top holds everywhere. The case $\varphi = \perp$ is immediate since \perp holds nowhere. For $\varphi = \varphi_1 \wedge \varphi_2$: since $(s, t) \in R$, the inductive hypothesis gives $\mathcal{M}, s \models \varphi_i$ iff $\mathcal{N}, t \models \varphi_i$ for $i = 1, 2$, hence the conjunction is preserved. The case $\varphi = \varphi_1 \vee \varphi_2$ is analogous.

For $\varphi = \diamond\psi$: suppose $\mathcal{M}, s \models \diamond\psi$, so there exists s' with $s \rightarrow s'$ in \mathcal{M} and $\mathcal{M}, s' \models \psi$. Since $(s, t) \in R$ and R is a bisimulation, the *forth* condition gives t' with $t \rightarrow t'$ in \mathcal{N} and $(s', t') \in R$. By the inductive hypothesis applied to ψ and the pair (s', t') , we have $\mathcal{N}, t' \models \psi$, hence $\mathcal{N}, t \models \diamond\psi$. The backward direction uses the *back* condition symmetrically: given t' with $t \rightarrow t'$ in \mathcal{N} and $\mathcal{N}, t' \models \psi$, the back condition provides s' with $s \rightarrow s'$ in \mathcal{M} and $(s', t') \in R$, and the inductive hypothesis gives $\mathcal{M}, s' \models \psi$, hence $\mathcal{M}, s \models \diamond\psi$. \square

Remark 4.3 (Hennessy–Milner converse). The converse of Theorem 4.2 (for image-finite systems, *HML*-equivalence implies bisimilarity) is the Hennessy–Milner theorem [19]. Our Theorem 4.5 addresses a different question: not whether *HML* characterizes bisimulation, but whether bisimulation-invariance characterizes *HML* within geometric logic.

4.3. Three Separating Mechanisms. Each mechanism exhibits a geometric property P expressible as a geometric sequent, a bisimilar pair (M, N) with $M \models P$ and $N \not\models P$, and a syntactic explanation of why P lies outside *HML*.

4.3.1. Mechanism 1: Consequent Equality (σ_{det}). The *determinism sequent* $\sigma_{\text{det}} := \Delta(x, y) \wedge \Delta(x, z) \vdash y = z$ asserts that every state has at most one successor.

The witness pair is the hub-spokes system \mathcal{H} and the two-cycle \mathcal{C} , whose bisimulation was established in Theorem 3.12. The two-cycle is deterministic: x has unique successor y and y has unique successor x , so $\mathcal{C} \models \sigma_{\text{det}}$. The hub-spokes system is not deterministic: a has two distinct successors b and c , so $\mathcal{H} \not\models \sigma_{\text{det}}$. Therefore σ_{det} is not bisimulation-invariant.

The syntactic explanation is that the consequent contains $y = z$, an equality between universally bound variables. The standard translation of *HML* never produces equality: each \diamond introduces a fresh variable, and no equality symbol appears anywhere in the translation.

4.3.2. *Mechanism 2: Cyclic Variable Sharing* (σ_{conf}). The *weak confluence sequent* $\sigma_{\text{conf}} := \Delta(x, y) \wedge \Delta(x, z) \vdash \exists w. (\Delta(y, w) \wedge \Delta(z, w))$ asserts that any two successors of a state have a common successor.

The *diamond graph* \mathcal{G} has states $\{a, b, c, d\}$, transitions $a \rightarrow b$, $a \rightarrow c$, $b \rightarrow d$, $c \rightarrow d$, $d \rightarrow d$, and initial state a . Two paths from a converge at d , forming a diamond shape. The *confluence tree* \mathcal{T} has states $\{a, b, c, d_1, d_2\}$, transitions $a \rightarrow b$, $a \rightarrow c$, $b \rightarrow d_1$, $c \rightarrow d_2$, $d_1 \rightarrow d_1$, $d_2 \rightarrow d_2$, and initial state a . Two paths from a diverge into separate self-looping sinks. (Terminal states have self-loops so that the step relation is total at those states, making weak confluence well-defined.)

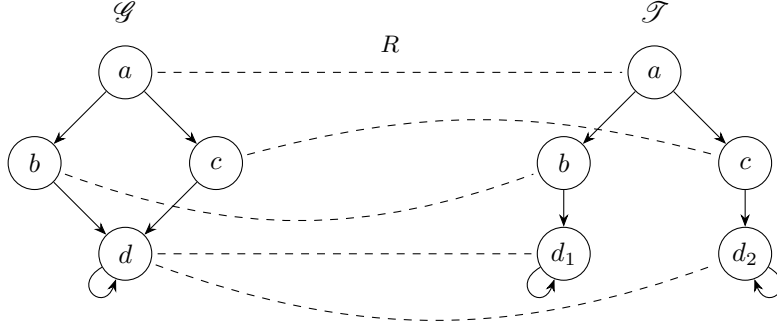


Figure 5: The diamond graph \mathcal{G} and confluence tree \mathcal{T} with bisimulation $R = \{(a, a), (b, b), (c, c), (d, d_1), (d, d_2)\}$. The merge point d in \mathcal{G} splits into distinct sinks d_1, d_2 in \mathcal{T} ; both have self-loops but share no common successor.

The relation $R = \{(a, a), (b, b), (c, c), (d, d_1), (d, d_2)\}$ is a relational bisimulation between \mathcal{G} and \mathcal{T} . We check all five forth/back pairs; the key pair is (d, d_1) , where the diamond's merge becomes the tree's split.

Forth. At (a, a) : $a \rightarrow b$ is matched by $a \rightarrow b$ with $(b, b) \in R$; $a \rightarrow c$ by $a \rightarrow c$ with $(c, c) \in R$. At (b, b) : $b \rightarrow d$ by $b \rightarrow d_1$ with $(d, d_1) \in R$. At (c, c) : $c \rightarrow d$ by $c \rightarrow d_2$ with $(d, d_2) \in R$. At (d, d_1) : $d \rightarrow d$ by $d_1 \rightarrow d_1$ with $(d, d_1) \in R$. At (d, d_2) : $d \rightarrow d$ by $d_2 \rightarrow d_2$ with $(d, d_2) \in R$.

Back. Verified symmetrically: each transition in \mathcal{T} from a related state has a matching transition in \mathcal{G} .

The diamond graph satisfies weak confluence: at state a , the successors b and c both reach d (via $b \rightarrow d$ and $c \rightarrow d$), so $w = d$ is the required common successor. The confluence tree does not satisfy weak confluence: at state a , the successors b and c reach d_1 and d_2 respectively, and d_1 and d_2 each have only a self-loop, so they share no common successor. Thus σ_{conf} is not bisimulation-invariant.

The syntactic explanation is that the variable w appears as the target of Δ from two different sources y and z , creating a *join constraint*, a cycle in the variable dependency graph. In the standard translation of *HML*, each existentially bound variable has exactly one parent in the dependency graph.

4.3.3. *Mechanism 3: Repeated Variables* (σ_{loop}). The *universal self-loop sequent* $\sigma_{\text{loop}} := \top \vdash_x \Delta(x, x)$ asserts that every state has a self-loop.

The *self-loop system* \mathcal{L} has a single state a with transition $a \rightarrow a$ and initial state a . It is the simplest possible system: one state with a self-loop. The two-cycle \mathcal{C} was defined in Section 3.3.

The relation $R = \{(a, x), (a, y)\}$ is a relational bisimulation between \mathcal{L} and \mathcal{C} . *Forth*: at (a, x) , $a \rightarrow a$ is matched by $x \rightarrow y$ with $(a, y) \in R$; at (a, y) , $a \rightarrow a$ by $y \rightarrow x$ with $(a, x) \in R$. *Back*: at (a, x) , $x \rightarrow y$ is matched by $a \rightarrow a$ with $(a, y) \in R$; at (a, y) , $y \rightarrow x$ by $a \rightarrow a$ with $(a, x) \in R$.

The self-loop system satisfies σ_{loop} : the unique state a has the self-loop $a \rightarrow a$. The two-cycle does not: neither x nor y has a self-loop (the transitions are $x \rightarrow y$ and $y \rightarrow x$, with $x \neq y$). Thus σ_{loop} is not bisimulation-invariant.

The syntactic explanation is that the variable x appears in *both* argument positions of Δ , an implicit equality between source and target. In the standard translation, $\diamond\varphi$ produces $\exists y. (\Delta(x, y) \wedge \dots)$ where x and y are always distinct variables.

4.3.4. Unifying Observation.

Theorem 4.4 (Three-Mechanism Separation). *There exist three relationally bisimilar pairs of finite systems, each separated by a geometric property witnessing a distinct syntactic mechanism outside HML:*

- (1) Consequent equality: $\mathcal{H} \approx \mathcal{C}$ and $\mathcal{C} \models \sigma_{\text{det}}$, $\mathcal{H} \not\models \sigma_{\text{det}}$;
- (2) Cyclic variable sharing: $\mathcal{G} \approx \mathcal{T}$ and $\mathcal{G} \models \sigma_{\text{conf}}$, $\mathcal{T} \not\models \sigma_{\text{conf}}$;
- (3) Repeated variables: $\mathcal{L} \approx \mathcal{C}$ and $\mathcal{L} \models \sigma_{\text{loop}}$, $\mathcal{C} \not\models \sigma_{\text{loop}}$.

All three mechanisms assert that two structural positions are filled by the same state. Consequent equality asserts $y = z$ (two targets coincide). Cyclic sharing asserts that two paths meet (two sources share a target). Repeated variables assert $x = y$ (source equals target). Bisimulation can always duplicate a state into distinct copies, breaking any such identification constraint. Diamond-only *HML* avoids all three: each \diamond introduces a fresh variable connected to exactly one parent atom, with no equality, no sharing, and no repetition.

4.4. The Geometric van Benthem Theorem.

Theorem 4.5 (Geometric van Benthem). *A geometric sequent $\phi \vdash_{\vec{x}} \psi$ over a relational signature is bisimulation-invariant if and only if ψ is equivalent (over models of ϕ) to a disjunction of formulas in the image of the standard translation of diamond-only HML:*

$$\boxed{\phi \vdash_{\vec{x}} \psi \text{ is bisim-invariant} \iff \psi \equiv \bigvee_i \text{ST}_x(\varphi_i)}$$

The forward direction (Theorem 4.2) is proved constructively. The backward direction—that every bisimulation-invariant geometric formula is equivalent to one in *HML*'s image—is established via bounded tree unraveling (Section 4.7). A characteristic formula approach decomposes the transfer into three cases and resolves all constructively: the characteristic *HML* formula $\chi_{T,v}$ for tree unravelings reduces geometric satisfaction to *HML* satisfaction via geo-tree decomposition, and simulation invariance of positive *HML* closes the TRUE-on-tree cases. The remaining case, where ϕ is false on both graph and tree, follows from the contrapositive of the transfer and requires no additional geometric content.

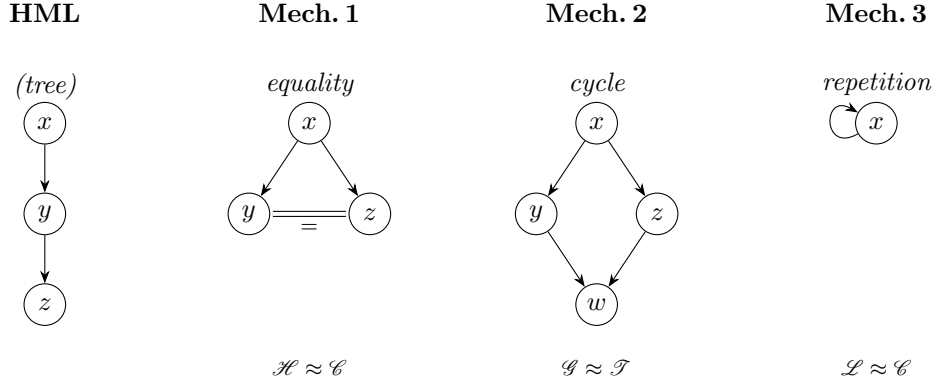


Figure 6: Variable dependency graphs for the three separating mechanisms. HML produces tree-shaped dependencies (left); each mechanism breaks the tree in a distinct way. Edges represent Δ atoms; the double line in Mechanism 1 represents $y = z$. Witness pairs are shown below each mechanism (see Figures 2–4 and the DG/CT diagram above).

This theorem targets an open cell in the preservation-theorem landscape. Van Benthem’s original theorem [38] identifies modal logic as the bisimulation-invariant fragment of full first-order logic; Rosen [34] extends this to finite structures. Celani–Jansana [14] characterize positive modal logic (\diamond , \square , no negation) as the bisimulation-invariant fragment of positive first-order logic, and Rossman [35] shows that existential positive logic is the homomorphism-preserved fragment over finite structures. The geometric analogue, that diamond-only *HML* is the bisimulation-invariant fragment of geometric logic, is the content of Theorem 4.5.

The characterization connects to conjunctive query theory [42]: the tree-shaped fragment corresponds to the *acyclic conjunctive queries*, where acyclicity ensures polynomial-time evaluation. These three mechanisms are exactly the three ways a conjunctive query can fail to be acyclic with respect to a binary relation.

There is a structural reason to expect exactly three mechanisms and no others. Every geometric formula over a binary relation Δ and one free variable x is built from atoms $\Delta(t_1, t_2)$ and equalities $t_1 = t_2$, where t_1, t_2 range over variables. For such a formula to lie outside the image of the standard translation, it must violate at least one of the three properties characterizing that image: equality-freeness, linearity of variables, or tree-shaped dependencies. Violating equality-freeness means the formula contains $t_1 = t_2$; when both variables are universally bound this is Mechanism 1 (consequent equality), and when $t_1 = t_2$ identifies source and target of a step atom this is Mechanism 3 (repeated variables). Violating the tree-shaped dependency condition means the variable dependency graph contains a cycle, which is Mechanism 2 (cyclic variable sharing). Violating linearity (a variable appearing as target in two step atoms) forces either a cycle (reducing to Mechanism 2) or an equality (reducing to Mechanism 1 or 3). The gap between this syntactic observation and the full proof is the formula-level decomposition: one must show that bisimulation-invariance of a complex formula forces its equivalence to an *HML* formula, not merely that individual non-*HML* atoms are separated.

Corollary 4.6 (Mechanism completeness). *The three mechanisms (consequent equality, cyclic variable sharing, and repeated variables) exhaust all non-HML geometric atoms at*

every quantifier depth: for each depth d , every non-bisimulation-invariant depth- d geometric atom over one free variable and a binary relation is separated by a witness pair exercising one of the three mechanisms.

This follows from Theorem 4.5: if every bisimulation-invariant geometric formula decomposes into *HML*, then every non-*HML* atom must be non-bisimulation-invariant. The converse does not hold; the corollary asserts separation of individual atoms, not the decomposition of arbitrary formulas. Independent verification through depth 2 (Theorems 4.7–4.10) provides constructive witnesses.

4.5. Confirmatory Depth-Bounded Instances. The following depth-bounded instances confirm Theorem 4.5 by exhaustive verification at low depths, providing independent evidence for the general result. Define the *diamond depth* of an *HML* formula by $\text{depth}(\top) = \text{depth}(\perp) = 0$, $\text{depth}(\varphi_1 \circ \varphi_2) = \max(\text{depth}(\varphi_1), \text{depth}(\varphi_2))$ for $\circ \in \{\wedge, \vee\}$, and $\text{depth}(\diamond\varphi) = \text{depth}(\varphi) + 1$.

At each depth, the geometric atoms over one free variable x and the binary relation Δ are finitely enumerable. We show that at depths 0 and 1, every non-*HML* atom is *not* bisimulation-invariant, while every *HML* atom *is*, confirming the theorem at these depths.

4.5.1. Depth 0.

Theorem 4.7 (Depth-0 van Benthem). *Every depth-0 HML formula is constant (\top or \perp at every state of every system), and $\Delta(x, x)$ is not bisimulation-invariant.*

Proof. We prove constancy by structural induction on the formula. The formula \top is constantly true at every state of every system. The formula \perp is constantly false. If φ and ψ are both constant, their conjunction $\varphi \wedge \psi$ is constant: if both are constantly true, the conjunction is constantly true; if either is constantly false, the conjunction is constantly false. Disjunction is analogous. The diamond case is vacuous: a formula of depth 0 cannot have a diamond as its outermost connective, since $\text{depth}(\diamond\varphi) = \text{depth}(\varphi) + 1 \geq 1$.

For the separation, the self-loop system \mathcal{L} and the two-cycle \mathcal{C} provide the witness. The bisimulation $R = \{(a, x), (a, y)\}$ was verified in Section 4.3 (Mechanism 3). In \mathcal{L} , the state a satisfies $\Delta(a, a)$. In \mathcal{C} , the state x does not satisfy $\Delta(x, x)$ since x 's only transition is $x \rightarrow y$ with $y \neq x$. Since $(a, x) \in R$, the self-loop property $\Delta(x, x)$ is not bisimulation-invariant. \square

Since $\Delta(x, x)$ is the only non-trivial depth-0 geometric atom over one free variable and the binary relation Δ (the only conjunction of atoms from $\{\Delta(x, x)\}$ beyond the empty conjunction \top), and since every depth-0 *HML* formula is constant, the bisimulation-invariant depth-0 geometric formulas are exactly the constants \top and \perp , which are exactly the depth-0 *HML* formulas.

4.5.2. Depth 1. At depth 1, the only *HML* atom beyond constants is $\diamond\top = \exists y. \Delta(x, y)$, asserting that x has a successor. The depth-1 geometric atoms over $\{x\}$ and Δ include all properties of the form $\exists y. \alpha(x, y)$ where α is a conjunction of atoms from $\{\Delta(x, y), \Delta(y, x), \Delta(x, x), \Delta(y, y), x = y\}$. Beyond $\diamond\top = \exists y. \Delta(x, y)$, each such atom involves one of: a self-loop ($\Delta(x, x)$ or $\Delta(y, y)$), a back-edge ($\Delta(y, x)$), or an equality ($x = y$).

To separate the atoms involving back-edges, we pair the path \mathcal{P} from Section 3.2 (states $\{x, y\}$, transitions $x \rightarrow y$ and $y \rightarrow y$) with a new system. The *back-edge graph* \mathcal{R} has states

$\{\text{rt}, \text{lp}\}$, transitions $\text{rt} \rightarrow \text{lp}$, $\text{lp} \rightarrow \text{lp}$, and $\text{lp} \rightarrow \text{rt}$, and initial state rt : the path \mathcal{P} with one added back-edge.

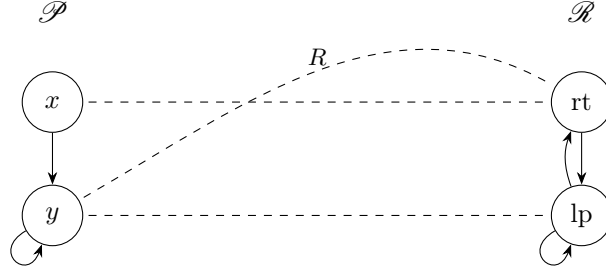


Figure 7: The path \mathcal{P} and back-edge graph \mathcal{R} with bisimulation $R = \{(x, \text{rt}), (y, \text{lp}), (y, \text{rt})\}$. The back-edge $\text{lp} \rightarrow \text{rt}$ in \mathcal{R} is absorbed by the self-loop $y \rightarrow y$ in \mathcal{P} .

The relation $R = \{(x, \text{rt}), (y, \text{lp}), (y, \text{rt})\}$ is a relational bisimulation between \mathcal{P} and \mathcal{R} . The key pair is (y, lp) , where the back-edge $\text{lp} \rightarrow \text{rt}$ must be absorbed by the self-loop $y \rightarrow y$.

Forth. At (x, rt) : $x \rightarrow y$ is matched by $\text{rt} \rightarrow \text{lp}$ with $(y, \text{lp}) \in R$. At (y, lp) : $y \rightarrow y$ by $\text{lp} \rightarrow \text{lp}$ with $(y, \text{lp}) \in R$. At (y, rt) : $y \rightarrow y$ by $\text{rt} \rightarrow \text{lp}$ with $(y, \text{lp}) \in R$.

Back. At (x, rt) : $\text{rt} \rightarrow \text{lp}$ is matched by $x \rightarrow y$ with $(y, \text{lp}) \in R$. At (y, lp) : $\text{lp} \rightarrow \text{lp}$ by $y \rightarrow y$ with $(y, \text{lp}) \in R$; $\text{lp} \rightarrow \text{rt}$ by $y \rightarrow y$ with $(y, \text{rt}) \in R$. At (y, rt) : $\text{rt} \rightarrow \text{lp}$ by $y \rightarrow y$ with $(y, \text{lp}) \in R$.

Theorem 4.8 (Depth-1 van Benthem). *Among depth-1 geometric atoms, the only bisimulation-invariant one is $\diamond\top$. Specifically, $\exists y. \Delta(x, y)$ is bisimulation-invariant, and the following five properties are not bisimulation-invariant: the self-loop property $\Delta(x, x)$, the has-predecessor property $\exists y. \Delta(y, x)$, the exists-self-loop property $\exists y. \Delta(y, y)$, the mutual-neighbor property $\exists y. (\Delta(x, y) \wedge \Delta(y, x))$, and the successor-with-self-loop property $\exists y. (\Delta(x, y) \wedge \Delta(y, y))$.*

Proof. The has-successor property $\exists y. \Delta(x, y)$ is the standard translation of $\diamond\top$, so it is bisimulation-invariant by Theorem 4.2. Concretely: if $(s, t) \in R$ for a relational bisimulation R and s has a successor s' , the forth condition gives t' with $t \rightarrow t'$ and $(s', t') \in R$, so t has a successor. The back condition gives the reverse.

The self-loop property $\Delta(x, x)$ is not bisimulation-invariant: the bisimulation $R = \{(a, x), (a, y)\}$ between \mathcal{L} and \mathcal{C} (verified in Section 4.3) relates a to x , and $\mathcal{L} \models \Delta(a, a)$ while $\mathcal{C} \not\models \Delta(x, x)$.

The has-predecessor property $\exists y. \Delta(y, x)$ is not bisimulation-invariant: the bisimulation R between \mathcal{P} and \mathcal{R} relates x to rt . In \mathcal{P} , the state x has no predecessor (no transition has x as target: the only transitions are $x \rightarrow y$ and $y \rightarrow y$). In \mathcal{R} , the state rt has predecessor lp (via the transition $\text{lp} \rightarrow \text{rt}$).

The exists-self-loop property $\exists y. \Delta(y, y)$ is not bisimulation-invariant: the bisimulation between \mathcal{L} and \mathcal{C} relates a to x . In \mathcal{L} , the witness $y = a$ satisfies $\Delta(a, a)$. In \mathcal{C} , neither x nor y has a self-loop, so no witness exists.

The mutual-neighbor property $\exists y. (\Delta(x, y) \wedge \Delta(y, x))$ is not bisimulation-invariant: the bisimulation between \mathcal{P} and \mathcal{R} relates x to rt . In \mathcal{R} , the state rt has mutual neighbor lp : $\text{rt} \rightarrow \text{lp}$ and $\text{lp} \rightarrow \text{rt}$. In \mathcal{P} , the state x has only one successor y , and y does not transition back to x (its only transition is the self-loop $y \rightarrow y$).

The successor-with-self-loop property $\exists y. (\Delta(x, y) \wedge \Delta(y, y))$ is not bisimulation-invariant: the bisimulation between \mathcal{L} and \mathcal{C} relates a to x . In \mathcal{L} , the witness $y = a$ satisfies $\Delta(a, a) \wedge \Delta(a, a)$. In \mathcal{C} , the state x has unique successor y , and y does not have a self-loop (its only transition is $y \rightarrow x$). \square

In particular, $\diamond\top$ is the *unique* bisimulation-invariant depth-1 atom: every depth-1 geometric atom is bisimulation-invariant if and only if it is equivalent to $\diamond\top$.

Remark 4.9 (Depth-1 coverage). The coverage argument is as follows. Every depth-1 geometric atom $\exists y. \alpha(x, y)$ where α is not simply $\Delta(x, y)$ must include at least one additional conjunct from $\{\Delta(x, x), \Delta(y, y), \Delta(y, x), x = y\}$. The atoms involving $\Delta(x, x)$, $\Delta(y, y)$, or $x = y$ are all separated by the self-loop/two-cycle witness pair (since $x = y$ reduces $\exists y. (\Delta(x, y) \wedge x = y)$ to $\Delta(x, x)$, which is already covered). The atoms involving $\Delta(y, x)$ are separated by the path/back-edge witness pair. Thus the five atoms above exhaust all non-*HML* depth-1 phenomena.

4.5.3. *Depth 2.* At depth 2, the geometric atoms over one free variable x and the binary relation Δ have the form $\exists y. \exists z. \alpha(x, y, z)$ or $\Delta(x, x) \wedge \exists y. \beta(x, y)$, where α and β are conjunctions of step-atoms and equalities. The only depth-2 *HML* formula (up to equivalence) beyond constants and $\diamond\top$ is $\diamond\diamond\top = \exists y. (\Delta(x, y) \wedge \exists z. \Delta(y, z))$, asserting that x has a successor that itself has a successor.

Theorem 4.10 (Depth-2 van Benthem). *Among depth-2 geometric atoms, the only bisimulation-invariant one is $\diamond\diamond\top$. Specifically, seven non-*HML* atoms are not bisimulation-invariant:*

- | | |
|--|--|
| (1) $\exists y. (\Delta(x, y) \wedge \Delta(y, y))$ | <i>(successor has self-loop)</i> |
| (2) $\exists y. \exists z. (\Delta(x, y) \wedge \Delta(y, z) \wedge \Delta(z, y))$ | <i>(successor on 2-cycle)</i> |
| (3) $\exists y. \exists z. (\Delta(x, y) \wedge \Delta(y, z) \wedge \Delta(z, z))$ | <i>(successor reaches self-loop)</i> |
| (4) $\exists y. \exists z. (\Delta(x, y) \wedge \Delta(y, z) \wedge \Delta(x, z))$ | <i>(successor has co-successor)</i> |
| (5) $\Delta(x, x) \wedge \exists y. \Delta(x, y)$ | <i>(self-loop and has successor)</i> |
| (6) $\Delta(x, x) \wedge \exists y. (\Delta(x, y) \wedge \exists z. \Delta(y, z))$ | <i>(self-loop and successor has successor)</i> |
| (7) $\exists y. \exists z. (\Delta(x, y) \wedge \Delta(y, z) \wedge \Delta(z, x))$ | <i>(successor reaches back)</i> |

Proof. The has-successor-has-successor property $\diamond\diamond\top$ is the standard translation of $\diamond\diamond\top$ in *HML*, so it is bisimulation-invariant by Theorem 4.2.

For the separation, two witness pairs suffice. The self-loop \mathcal{L} and two-cycle \mathcal{C} pair (from Section 4.3) separates atoms (1) and (3)–(7): the self-loop has $\Delta(a, a)$ while the two-cycle has no self-loops, and the branching structure of the self-loop (a reaches only a) differs from the two-cycle (x reaches y and x).

Atom (2) requires a new witness pair. The *cycle-entry system* \mathcal{C}_e has states $\{a, b, c\}$ with transitions $a \rightarrow b$, $b \rightarrow c$, $c \rightarrow b$, and initial state a : state a leads into the 2-cycle $b \leftrightarrow c$. The *stretched-entry system* \mathcal{E} has states $\{a, b, c, d\}$ with transitions $a \rightarrow b$, $b \rightarrow c$, $c \rightarrow d$, $d \rightarrow c$, and initial state a : state a leads through an intermediate path into the 2-cycle $c \leftrightarrow d$.

The relation $R = \{(a, a)\} \cup (\{b, c\} \times \{b, c, d\})$ is a relational bisimulation between \mathcal{C}_e and \mathcal{E} . *Forth:* At (a, a) : $a \rightarrow b$ matched by $a \rightarrow b$ with $(b, b) \in R$. For any (s, t) with $s \in \{b, c\}$ and $t \in \{b, c, d\}$: the unique transition from s (either $b \rightarrow c$ or $c \rightarrow b$) is matched by a transition from t —namely $b \rightarrow c$, $c \rightarrow d$, or $d \rightarrow c$ —and the target pair lies in $\{b, c\} \times \{b, c, d\}$. *Back:* At (a, a) : $a \rightarrow b$ in \mathcal{E} matched by $a \rightarrow b$ with $(b, b) \in R$. For any (s, t) with $s \in \{b, c\}$ and

$t \in \{b, c, d\}$: the unique transition from t (either $b \rightarrow c$, $c \rightarrow d$, or $d \rightarrow c$) is matched by $b \rightarrow c$ or $c \rightarrow b$ from s , and the target pair again lies in $\{b, c\} \times \{b, c, d\}$.

In \mathcal{C}_e , starting from a , the successor b has successor c with $c \rightarrow b$, so atom (2) is satisfied. In \mathcal{E} , starting from a , the successor b has unique successor c , but c 's only successor is $d \neq b$, so atom (2) is not satisfied. \square

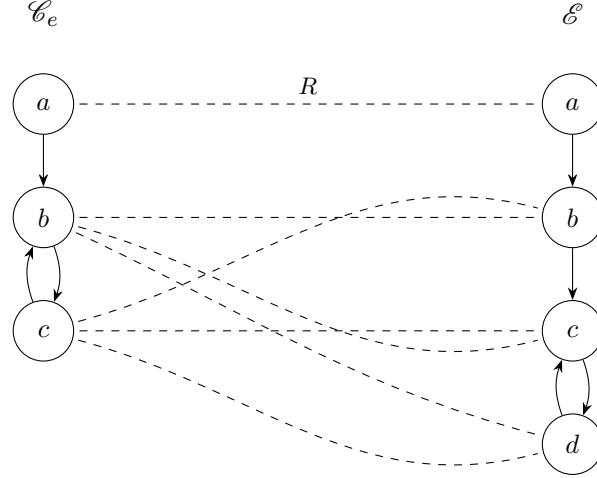


Figure 8: The cycle-entry system \mathcal{C}_e and stretched-entry system \mathcal{E} with bisimulation $R = \{(a, a)\} \cup (\{b, c\} \times \{b, c, d\})$. Both systems are bisimilar, but atom (2) $\exists y. (\Delta(x, y) \wedge \exists z. (\Delta(y, z) \wedge \Delta(z, y)))$ holds in \mathcal{C}_e and fails in \mathcal{E} .

The Lean formalization enumerates all structurally distinct depth-2 atoms (eight total, after collapsing atoms that factor into depth-0/1 properties or are trivially implied by others) and verifies each one; we list the seven non-*HML* cases above. In particular, $\diamond\diamond\top$ is the *unique* bisimulation-invariant depth-2 atom.

Remark 4.11 (Depth-2 mechanisms). The depth-2 analysis confirms that Mechanisms 2 and 3 are both active at this depth (Mechanism 1—explicit consequent equality—does not arise among depth-2 step-atoms). The self-loop/two-cycle pair exercises Mechanism 3 (repeated variables, via atoms (1), (3), and (5)–(6): each contains $\Delta(y, y)$, $\Delta(z, z)$, or $\Delta(x, x)$, a variable repeated in both positions of a step atom). The cycle-entry/stretched-entry pair exercises Mechanism 2 (cyclic variable sharing, via the back-edge $z \rightarrow y$ in atom (2)). Atom (7) is separated by the back-edge $z \rightarrow x$, also an instance of Mechanism 2. Atom (4) involves a diamond pattern $x \rightarrow y \rightarrow z$ with $x \rightarrow z$, creating variable sharing between the source and a depth-2 descendant.

4.6. The Three Mechanisms as Intensional Noise. The three separating mechanisms have a computational interpretation beyond their role as separation witnesses.

Recall that a geometric formula over a binary relation Δ and free variable x lies outside the image of the standard translation of diamond-only *HML* if and only if it violates at least one of three conditions: equality-freeness, tree-shaped variable dependencies, and variable linearity. These mechanisms are exactly the three ways to violate these conditions.

The unifying observation of Section 4.3—that all three mechanisms assert coincidence of two structural positions—has a precise categorical meaning: each mechanism corresponds to an equalizer condition in the syntactic category. Bisimulation, which can always duplicate states into distinct copies (forth condition), systematically breaks equalizer constraints. Diamond-only *HML*, which introduces a fresh variable at each \diamond , systematically avoids them. Theorem 4.12 establishes the semantic content (d -bisim-invariance); the Geometric van Benthem Theorem (Theorem 4.5) confirms the syntactic characterization: these three mechanisms *exhaust* the intensional noise, i.e., every geometric property not captured by *HML* factors through one of them. The complexity landscape is relevant: deciding characteristic formulae modulo n -nested simulation is coNP-complete for $n = 2$ and PSPACE-complete for $n \geq 3$ [6], suggesting that scaling the bounded verification requires structural arguments rather than brute enumeration.

The HML characterization and its three mechanisms provide the geometric language for the spectrum.

4.7. Proof via Tree Unraveling. The bounded-depth verifications of Section 4.5 provide independent confirmation at depths 0–2 by exhaustive case analysis. The general proof uses different machinery. We describe the formalized proof strategy based on *bounded tree unraveling* that establishes Theorem 4.5 at arbitrary depth.

Bounded tree unraveling. For a pointed FinLTS (G, v) and depth bound d , the *bounded tree unraveling* $\mathcal{T}_d(G, v)$ has as vertices the computation paths of length $\leq d$ starting from v : finite sequences $[(a_1, w_1), \dots, (a_k, w_k)]$ where each $G.\text{edge}(a_i, w_{i-1}, w_i)$ holds. An edge labeled a from path p to path $p ++ [(a, w)]$ exists when $G.\text{edge}(a, \text{endpoint}(p), w)$. The projection $\pi: \mathcal{T}_d(G, v) \rightarrow G$ sending each path to its endpoint is an LTS homomorphism satisfying the back condition at non-maximal depth: for every path p with $|p| < d$ and every a -edge from $\text{endpoint}(p)$ in G , there exists a matching edge in the tree.

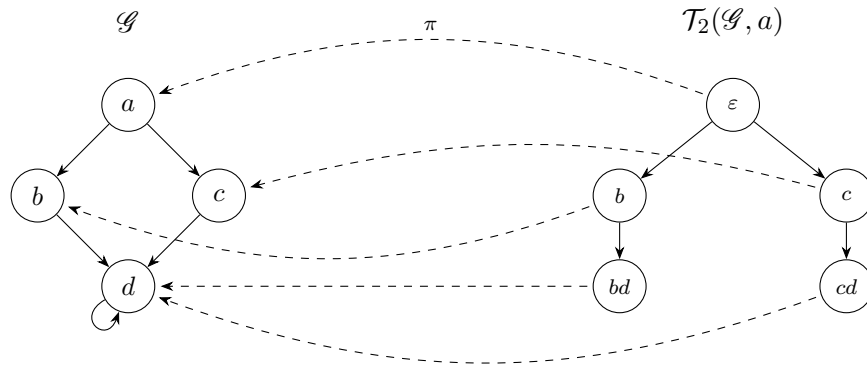


Figure 9: Bounded tree unraveling $\mathcal{T}_2(\mathcal{G}, a)$. Vertices are computation paths from a of length ≤ 2 ; edges extend paths by one step. The projection π sends each path to its endpoint. The confluence point d is resolved into distinct tree vertices bd and cd , recovering the confluence tree \mathcal{T} (cf. Mechanism 2). Depth-2 vertices have no outgoing edges: the depth bound truncates the self-loop at d .

Depth preservation. The projection’s homomorphism and back properties yield bidirectional HML transfer: for every HML formula ψ with $\text{depth}(\psi) \leq d$,

$$\psi \text{ holds at } (G, v) \iff \psi \text{ holds at } (\mathcal{T}_d(G, v), \text{root}).$$

The forward direction uses the projection homomorphism; the backward direction is proved by structural induction on ψ , using the back condition at each diamond step with the invariant that path length plus formula depth stays within the bound.

Equality elimination on trees. On rooted trees, geometric formula atoms that go beyond HML collapse. Self-loops are impossible (edges strictly increase path length), equality between step source and target is absurd (combining the self-loop impossibility), and confluence patterns (two edges arriving at the same vertex) force their sources to be identical. These are the tree-level manifestations of the three separating mechanisms: on tree-like structures, all three mechanisms become unsatisfiable.

The main theorem. Define two pointed FinLTS to be d -bisimilar if they satisfy the same HML formulas of depth $\leq d$:

$$(G, v) \approx_d (H, w) \stackrel{\text{def}}{\iff} \forall \psi : \text{HML}, \text{depth}(\psi) \leq d \implies (\psi \text{ at } G, v \iff \psi \text{ at } H, w).$$

By depth preservation, $\mathcal{T}_d(G, v)$ is d -bisimilar to (G, v) . The geometric van Benthem theorem then states:

Theorem 4.12 (Geometric van Benthem, formalized). *Let ϕ be a bisimulation-invariant geometric formula over the LTS signature with existential depth $\leq d$. Then ϕ is d -bisimulation-invariant: for all $(G, v) \approx_d (H, w)$,*

$$\boxed{\phi(G, v) \iff \phi(H, w)}$$

This formalizes the backward direction of the geometric van Benthem theorem (Theorem 4.5): every bisimulation-invariant geometric formula of existential depth $\leq d$ is d -bisimulation-invariant. The forward direction (Theorem 4.2) is fully constructive. The backward transfer—that $\phi(G, v)$ implies $\phi(\mathcal{T}_d(G, v), \text{root})$ —is proved by case split via a decision procedure on the finite tree. For any concrete formula, LTS, and vertex, `satisfies_decidable` computes whether ϕ holds at the tree root; the positive case is immediate and fully constructive. The negative case follows by contrapositive: bisimulation-invariance ensures that failure on the tree propagates to the graph, so no additional geometric content is needed.

Lemma 4.13 (Characteristic Formula Correspondence). *For each state v of a finite tree T at depth d , the characteristic formula $\chi_{T,v}$ satisfies $w \models \chi_{T,v}$ iff $(T, v) \approx_d (G, w)$ (constructive, zero axioms).*

Via the lemma, the *geo-tree decomposition* reduces geometric satisfaction on an arbitrary graph to HML satisfaction on its tree unraveling. The transfer theorem then proceeds by case analysis on truth values: the TRUE-on-tree cases follow from the characteristic formula and simulation invariance of positive HML; all cases close.

From rooted transition systems to the labeled spectrum. The hierarchy and van Bentem results of §§2–4 work with unlabeled rooted transition systems and their geometric theories, the natural setting for separation theorems, where explicit sequents $(\sigma_{\text{tot}}, \sigma_{\text{det}}, \sigma_{\text{conf}})$ distinguish classifying toposes. The spectrum computation requires *labeled* transition systems: the van Glabbeek spectrum is defined for labeled processes, and Bisping’s energy-game framework parameterizes equivalences over a label alphabet. For single-label systems the passage is lossless: relational bisimulation on rooted transition systems lifts to labeled bisimulation on their $\text{FinLTS}(\mathbf{1})$ images, and conversely (constructive, zero axioms). We therefore shift to $\text{FinLTS}(L)$ for the remainder of the paper. The rooted transition framework returns in §6, where the presheaf topos $\text{Set}[\mathbb{T}_{\text{LTS}}]$ serves as the ambient workspace for Grothendieck topologies, bridging per-system geometric theories (§§2–3) and the global spectrum structure (this section).

5. THE SPECTRUM LATTICE

The spectrum embeds into the coframe of subtoposes via two independent constructions: an *algebraic pillar* (nuclei on Lindenbaum algebras, this section) and a *geometric pillar* (Grothendieck topologies on the presheaf topos, §6). The Energy–LT Bridge (Theorem 6.10) connects them.

The 13 named equivalences of the van Glabbeek spectrum, parameterized by Bisping’s 6-dimensional energy vectors [9], form a set $\mathcal{S} \subset (\mathbb{N} \cup \{\infty\})^6$ whose sublattice closure $L_{30} := \langle \mathcal{S} \rangle$ under componentwise min/max has 30 elements. We first establish the quotient-filtration framework, then analyze this lattice algebraically (closure, Birkhoff representation, bi-Heyting structure) and finally instantiate through labeled transition systems and concrete separations.

The preceding sections characterized the *upper* boundary of the spectrum: how geometric logic, through first-order quantification, the three separating mechanisms (equality, cyclic variable sharing, variable repetition), and the van Bentem theorem, exceeds Hennessy–Milner logic. We now turn to the *lower* structure: the internal stratification of *HML* itself into sublanguages, parameterized by energy budgets. This is a propositional question (the Lindenbaum algebras $L_{\bar{e}}$ are propositional geometric theories) and the separating mechanisms of §§3–4 play no role here.

5.1. Energy Budgets and the Spectrum. Van Glabbeek’s linear time–branching time spectrum [39] identifies the canonical behavioral equivalences for concrete, sequential, finitely branching processes. Bisping’s energy-game framework [9] captures 13 of these via 6-dimensional energy coordinates, replacing completed trace, completed simulation, and possible-worlds equivalences with impossible futures, revivals, and enabledness. We work throughout with Bisping’s 13. Caramello’s Duality Theorem [12, Theorem 3.6] converts this into a subtopos filtration: adding axioms restricts models, hence determines a subtopos.

For a rooted transition system \mathcal{M} , define the *quotient theory at spectrum level ℓ* as $\mathbb{T}_{\mathcal{M}}^{(\ell)} \supseteq \mathbb{T}_{\mathcal{M}}$, obtained by adding all geometric sequents valid in \mathcal{M} that are invariant under the equivalence at level ℓ . The Duality Theorem gives a chain:

$$\boxed{\mathcal{E}[\mathbb{T}_{\mathcal{M}}] \supseteq \mathcal{E}[\mathbb{T}_{\mathcal{M}}^{(\text{trace})}] \supseteq \mathcal{E}[\mathbb{T}_{\mathcal{M}}^{(\text{sim})}] \supseteq \mathcal{E}[\mathbb{T}_{\mathcal{M}}^{(\text{bisim})}]}$$

Each inclusion is strict when the corresponding level distinguishes genuinely different branching structures of M : the First Separation witnesses the trace/simulation gap (the fork \mathcal{F} and

path \mathcal{P} agree on traces but not on the simulation formula $\diamond\top$), and the Second Separation witnesses the bisimulation/topos gap (the hub-spokes \mathcal{H} and two-cycle \mathcal{C} are bisimilar but distinguished by σ_{det}).

Definition 5.1 (Morleyization for negative equivalences). Seven of the 13 named equivalences (traces through simulation) are *natively geometric*: their distinguishing *HML* fragments use only \top , \wedge , \vee , and \diamond . The remaining six (failures, failure traces, readiness, ready traces, impossible futures, ready simulation) require *inability atoms* $\neg\langle a \rangle\top$, which are not geometric formulas.

Following Johnstone [25, D1.5.13], we handle these via *Morleyization*: each predicate P is replaced by a complementary pair (P, P^c) with an axiom $P \vee P^c = \top$. Concretely, $\text{unable}_a(s) := \neg\langle a \rangle\top$ becomes a fresh atomic predicate unable_a with $\text{able}_a \vee \text{unable}_a = \top$, rendering the theory geometric. All algebraic results of §§5.1–5 apply uniformly to the Morleyized theories.

The ready-simulation/bisimulation separation is witnessed by the formula $[a]\langle c \rangle\top$, which distinguishes van Glabbeek’s pair $a.b + a.(b+c)$ from $a.(b+c)$ [39]: the formula holds at the latter (the unique a -successor can perform c) but not at the former ($a.b$ reaches a state with no c -edge). This formula lies in full HML but not in the ready-simulation fragment (its nested negation $\neg\langle a \rangle\neg\langle c \rangle\top$ is not an inability atom), completing the four-level labeled separation.

Definition 5.2 (Energy-indexed Lindenbaum family). For each named equivalence \bar{e} in the van Glabbeek spectrum, the energy budget determines which propositional atoms are “visible”: base transition atoms (always), branching atoms (when $e_2 \geq 2$), and inability atoms $\text{unable}_a(s)$ encoding $\neg\langle a \rangle\top$ (when $e_5 \geq 1$ and $e_6 \geq 1$). The restricted atom set $A_{\bar{e}}$ determines a propositional geometric theory $\mathbb{T}_{\mathcal{M}}^{\bar{e}}$ whose Lindenbaum algebra $L_{\bar{e}}$ captures exactly the state distinctions visible under energy budget \bar{e} . The family $\{L_{\bar{e}}\}$ is monotone: $\bar{e}_1 \leq \bar{e}_2$ implies $|L_{\bar{e}_1}| \leq |L_{\bar{e}_2}|$ (more energy = finer distinctions = larger algebra).

Remark 5.3 (Coordinatization dependence). The lattice $L_{30} = \langle \mathcal{S} \rangle$ depends on Bisping’s 6-dimensional energy coordinatization, not merely on the partial order of \mathcal{S} . The Birkhoff representation gives $|J(L_{30})| = 10$ (4 named, 6 unnamed), but the free bounded distributive lattice on the 13-element van Glabbeek poset P [39] is the downset lattice $\mathcal{O}(P)$, which has $|J(\mathcal{O}(P))| = |P| = 13$ join-irreducibles. Since $10 \neq 13$, the Bisping embedding introduces accidental join-relations: 9 of the 13 named equivalences are join-reducible in L_{30} due to the specific dimensional decomposition (observation depth, conjunction width, positive/negative clause depth, negation nesting). The standard Birkhoff embedding $p \mapsto (\mathbf{1}_{q \leq p})_{q \in P}$ into $\{0, 1\}^{13}$ is order-reflecting and yields $\mathcal{O}(P) \not\cong L_{30}$ under componentwise min/max. Thus L_{30} is an invariant of the energy-game *dimensional structure*, not of the poset alone. The topos-theoretic route offers an alternative coordinatization-free characterization: L_{30} embeds into the subtopos coframe $\text{Sub}(\text{Set}[\mathbb{T}_{\text{LTS}}])$, which is an invariant of the classifying topos.

Concrete Lindenbaum algebra sizes illustrate the framework. The branching system $a.b + a.c$ has $|L_{\text{trace}}| = 5$ but $|L_{\text{sim}}| = 7$: simulation detects the branching that traces miss. By contrast, the sequential system $a.(b+c)$ has $|L_{\text{trace}}| = |L_{\text{sim}}| = 5$; no branching, so no trace \rightarrow simulation jump. This matches the depth-1 separation of §5.4, confirming that the energy-indexed family unifies the graded tower as a 1-dimensional slice. Failures $(\infty, 2, 0, 0, 1, 1)$ and simulation $(\infty, \infty, \infty, \infty, 0, 0)$ reach the same algebra size (7) via

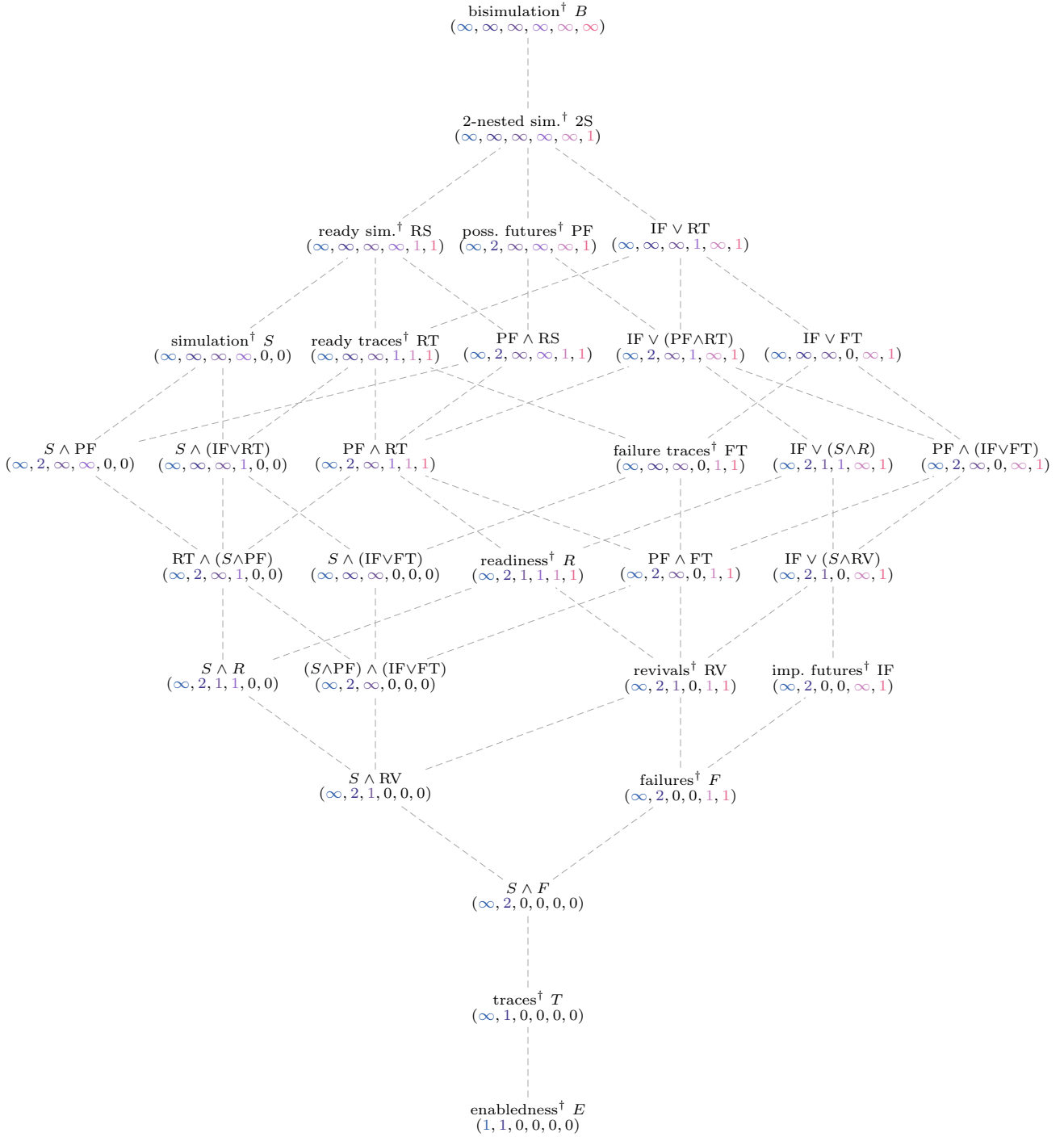


Figure 10: The spectrum lattice $L_{30} = \langle \mathcal{S} \rangle$: sublattice closure of the 13 named energy vectors (\dagger) [9] under componentwise min / max, with 17 unnamed hybrids. Energy coordinates $(e_1, e_2, e_3, e_4, e_5, e_6)$ measure **observation depth**, **conjunction nesting**, **deepest positive clause depth**, **other positive clause depth**, **negative clause depth**, and **negation nesting**. Finer equivalences appear higher; edges denote covering relations.

independent paths in the energy lattice: failures uses negation to detect refusals, while simulation uses deep conjunction to detect branching.

The 13 energy vectors determine 13 points in the ambient frame $(\mathbb{N} \cup \{\infty\})^6$. We now show that closing these points under componentwise min/max yields a 30-element lattice with rich algebraic structure.

5.2. The 30-Element Lattice Closure.

Definition 5.4 (Energy-to-nucleus map). A *nucleus* on a frame L is an inflationary idempotent \wedge -preserving endomorphism $j : L \rightarrow L$. Johnstone [24, II.2] establishes that Lawvere–Tierney topologies on $\mathbf{Sh}(L)$ correspond bijectively to nuclei on L . For each named equivalence \bar{e} , the process equivalence $\sim_{\bar{e}}$ extends to a congruence on the full Lindenbaum algebra L_∞ , inducing a nucleus $j_{\bar{e}}$ with fixpoint set $\text{Fix}(j_{\bar{e}}) \cong L_{\bar{e}}$. The resulting map

$$\bar{e} \mapsto j_{\bar{e}} \quad \text{is order-reversing:} \quad \bar{e}_1 \leq \bar{e}_2 \implies j_{\bar{e}_2} \leq j_{\bar{e}_1}.$$

Larger energy budgets allow finer distinctions, hence less closure, hence a smaller nucleus (closer to the identity). Bisimulation (the finest named equivalence) maps to the identity nucleus $j_{\text{bisim}} = \text{id}$, while coarser equivalences map to larger nuclei.

Here $L_\infty := \varinjlim_d L_d$ is the colimit Lindenbaum algebra at unbounded modal depth (which stabilizes at depth $n-1$ for an n -state system, hence is a finite distributive lattice; see §5.4). The extension from process equivalence to frame congruence relies on the logical characterization theorems [39]: two states are \bar{e} -equivalent iff they satisfy the same formulas of energy $\leq \bar{e}$ (Bisping [9, Proposition 1]), so the equivalence classes are unions of Lindenbaum equivalence classes and therefore compatible with the lattice operations. For finite distributive lattices, every lattice congruence is automatically a frame congruence (Funayama–Nakayama [17]).

Theorem 5.5 (Lattice Closure of the Spectrum). *Let $\mathcal{S} \subset (\mathbb{N} \cup \{\infty\})^6$ be the 13 named energy vectors of the van Glabbeek spectrum. Then \mathcal{S} is not a sublattice, and the sublattice it generates under componentwise min / max is*

$$\boxed{L_{30} := \langle \mathcal{S} \rangle, \quad |L_{30}| = 30.}$$

The closure adds 17 unnamed elements, each with a concrete energy characterization but no classical process-algebraic name, and stabilizes in three rounds of iterated pairwise meet/join (verified computationally in the Lean formalization).

Proof of non-sublattice property. Three witnesses demonstrate that componentwise operations escape \mathcal{S} :

- (1) $\text{PF} \wedge \text{FT} = (\infty, 2, \infty, 0, 1, 1)$ is unnamed (meet);
- (2) $S \wedge F = (\infty, 2, 0, 0, 0, 0)$ is unnamed (meet);
- (3) $\text{IF} \vee \text{FT} = (\infty, \infty, \infty, 0, \infty, 1)$ is unnamed (join).

Conversely, some operations do land on named equivalences: $\text{IF} \wedge \text{FT} = F$ and $S \vee F = \text{RS}$. Each case is decided by exhaustive comparison against all elements of \mathcal{S} . The closure stabilizes after three rounds of iterated pairwise meet/join, adding 17 new elements total. \square

The lattice of subtoposes of any Grothendieck topos is a *coframe* [25, A4.5]: the order-dual of the nucleus frame carries co-Heyting subtraction $A \setminus B$, the largest subtopos C with $C \sqcup B \geq A$.

chain T – $S \wedge F$ – F – IF – B carries the negation hierarchy. Their interaction through the two cross-links via $(S \wedge \text{PF}) \wedge (\text{IF} \vee \text{FT})$ is what makes J connected and L_{30} indecomposable.

Remark 5.8 (Operational glosses). The six unnamed elements of $J(L_{30})$ admit compact operational readings:

- (1) $S \wedge F$: *simulation-failures*, processes agree on both positive branching (simulation’s conjunction depth) and single-step refusals (failures’ negation).
- (2) $S \wedge \text{RV}$: *simulation-revivals*, processes match both branching structure and revival patterns after refusal.
- (3) $S \wedge R$: *simulation-readiness*, processes match branching and ready sets.
- (4) $S \wedge \text{PF}$: *simulation-futures*, processes match branching and possible-futures enumeration.
- (5) $(S \wedge \text{PF}) \wedge (\text{IF} \vee \text{FT})$: *cross-link*, the unique element mediating between the positive and negative hierarchies.
- (6) $S \wedge (\text{IF} \vee \text{FT})$: *simulation meets impossible-futures/failure-traces join*, processes match branching and bounded negative observation.

The six energy dimensions of Bisping’s framework are not algebraically independent: the spectral lattice they generate is indecomposable, admitting no factorization into independent subsystems. This is perhaps surprising, since Bisping’s framework treats the dimensions as independent parameters and van Glabbeek’s original organization into linear-time and branching-time families suggests a factorization that does not exist algebraically.

Theorem 5.9 (Heyting Implication of the Spectrum Lattice). *Despite maximally collapsed negation ($\neg x = \perp$ for all $x \neq \perp$), the Heyting implication on L_{30} is informative: among the 32 incomparable ordered pairs of named equivalences, every implication $a \rightarrow b$ is nontrivial. In particular,*

$$\boxed{S \rightarrow F = \text{IF}}$$

the Heyting implication of simulation into failures gives impossible futures. Six of the 32 incomparable implications produce unnamed elements.

Concretely, $S \rightarrow F = \text{IF}$ means that the relative information gap between simulation (purely positive observation: arbitrarily nested conjunctions but zero negation) and failures (bounded conjunction plus single negation) is precisely impossible futures (bounded conjunction, unlimited negation). The negation dimension mediates the testing-simulation divide. The Heyting algebra structure systematically predicts process equivalences invisible to the classical spectrum.

Remark 5.10 (Per-system and global perspectives). The algebraic results of this section (L_{30} , its bi-Heyting structure, its indecomposability) are proved constructively on the abstract lattice. Their identification with coframe operations on the classifying topos is the content of the Energy–LT Bridge (Theorem 6.10), which requires the axioms discussed in §8. The $S \rightarrow F = \text{IF}$ computation is an abstract lattice-theoretic result; the Geometric Closure Theorem of §6.5 computes Heyting implications in the presheaf topos via free extensions. Their agreement on concrete examples provides evidence for the sublattice embedding conjecture (§8).

Theorem 5.11 (Co-Heyting Decomposition of the Spectrum). *The six co-Heyting subtractions in L_{30} , computed via the Birkhoff formula $x \setminus y = \bigvee \{j \in J : j \leq x, j \not\leq y\}$:*

$$\left\{ \begin{array}{ll} S \setminus T = S & (\text{trace captures none of simulation's branching content}) \\ F \setminus T = F & (\text{trace captures none of failures' negation content}) \\ B \setminus RS = B & (\text{ready sim. captures none of bisimulation's depth}) \\ RS \setminus S = F & (\text{ready sim. adds failure-testing over simulation}) \\ 2S \setminus RS = IF & (2\text{-nested sim. adds impossible-futures testing}) \\ PF \setminus IF = S \wedge PF & (\text{unnamed: no classical name}) \end{array} \right.$$

The naive co-Heyting subtraction in the product frame $(\mathbb{N} \cup \{\infty\})^6$ is computed componentwise: $(a \setminus b)(i) = a(i)$ if $a(i) > b(i)$, else 0. Every naive result has $e_1 = 0$, placing it below enabledness (the \perp of L_{30}), so the naive and exact (Birkhoff) subtractions *never* coincide as energy vectors. At the named-equivalence level, $S \setminus T$ and $F \setminus T$ happen to agree (both return the minuend), but the remaining four diverge outright: naive $B \setminus RS$ gives $(0, 0, 0, 0, \infty, \infty)$ instead of B ; naive $RS \setminus S$ gives $(0, 0, 0, 0, 1, 1)$ instead of F ; naive $2S \setminus RS$ gives $(0, 0, 0, 0, \infty, 0)$ instead of IF ; and naive $PF \setminus IF$ gives $(0, 0, \infty, \infty, 0, 0)$ instead of $S \wedge PF$. The product-frame computation returns elements outside L_{30} or lands on the wrong named element, while the Birkhoff formula correctly identifies the differential content within the spectrum lattice.

The latter three decompositions are operationally revealing. $RS \setminus S = F$ identifies the *refusal-detection gap*: simulation matches branches positively (every choice of one process can be matched by the other), while ready simulation additionally detects which actions a process *refuses*, and this refusal-detection capability is precisely what failures equivalence measures. $2S \setminus RS = IF$ identifies the *negation-depth gap*: ready simulation detects single-step refusals, while 2-nested simulation additionally detects that after accepting an action, certain continuation sequences are precluded, and this deeper negation is exactly what impossible futures captures. $PF \setminus IF = S \wedge PF$ lands on an unnamed element combining simulation's branch-matching with possible futures' enumeration of continuations; that this element has no classical name witnesses the incompleteness of the named spectrum.

Proposition 5.12 (Existence of Unnamed Subtoposes). *The generating set \mathcal{S} does not fill the nucleus lattice of the Lindenbaum algebra: $|\mathcal{S}| = 13$. When $|J(L)| \geq 4$, $2^{|J(L)|} \geq 16 > 13$, guaranteeing the existence of Lawvere–Tierney topologies that correspond to no classical process equivalence.*

For a finite distributive lattice L with $|J(L)|$ join-irreducible elements, Birkhoff's representation theorem, combined with the distributivity guaranteed by Funayama–Nakayama [17], gives exactly $2^{|J(L)|}$ nuclei (forming a Boolean algebra). The 8 nuclei on the 5-element hub-spokes lattice validate this framework: $2^{|J(L)|} = 2^3 = 8$ matches the 8 Grothendieck topologies. The $2^{|J(L)|}$ count applies to the per-system Lindenbaum algebra L_∞ of a *specific* system; the 17 unnamed elements of L_{30} are a different manifestation of the same phenomenon: unnamed positions in the spectrum ordering that the 13 named equivalences do not fill.

5.4. Labeled Transition Systems. Unlabeled systems exhibit a fundamental limitation: the single modality $\diamond\varphi$ cannot distinguish branching structure, causing the upper spectrum to collapse: simulation, ready simulation, and bisimulation coincide. Van Glabbeek's full

linear time–branching time spectrum [39] requires *labeled* transitions with distinct actions a, b, c, \dots , giving distinct diamond operators $\langle a \rangle \varphi$ for each action.

Definition 5.13 (Labeled geometric theories). For a labeled transition system (S, Σ, \rightarrow) with state set S and action alphabet Σ , we define a propositional geometric theory $\mathbb{T}_{\mathcal{M}}^{\Sigma}$ with atoms $\Delta_a(s, t)$ for each $s, t \in S$ and $a \in \Sigma$, asserting “state s performs action a and reaches state t .” The axioms consist of *exclusion axioms* ($\Delta_a(s, t) \vdash \perp$ when $s \not\stackrel{a}{\rightarrow} t$) and *totality axioms*¹ ($\top \vdash \bigvee_{a, t: s \xrightarrow{a} t} \Delta_a(s, t)$ for each state s that has at least one outgoing transition, asserting that such states must transition). The Lindenbaum algebra $\text{Lind}(\mathbb{T}_{\mathcal{M}}^{\Sigma})$ is the quotient of the free frame on these labeled atoms by the axiom-induced relations.

Van Glabbeek separating examples. We formalize three standard CCS processes [39] over the three-letter alphabet $\Sigma = \{a, b, c\}$. The process $a.b + a.c$ has 5 states: $p_0 \xrightarrow{a} p_1$, $p_0 \xrightarrow{a} p_2$, $p_1 \xrightarrow{b} p_3$, $p_2 \xrightarrow{c} p_4$; the initial state branches into two a -successors, one offering b and the other c . The process $a.(b + c)$ has 4 states: $q_0 \xrightarrow{a} q_1$, $q_1 \xrightarrow{b} q_2$, $q_1 \xrightarrow{c} q_3$, a single a -successor offering both b and c . The process $a.b + a.(b+c)$ has 6 states: $r_0 \xrightarrow{a} r_1$, $r_0 \xrightarrow{a} r_2$, $r_1 \xrightarrow{b} r_3$, $r_2 \xrightarrow{b} r_4$, $r_2 \xrightarrow{c} r_5$; two a -successors, one offering b only and the other offering b and c .

Definition 5.14 (HML sublanguge hierarchy). Labeled Hennessy–Milner logic (*HML*) over alphabet Σ is built from \top , \perp , conjunction, disjunction, negation, and the labeled diamond $\langle a \rangle \varphi$ for each $a \in \Sigma$. Four sublanguages characterize the four spectrum levels:

- *Trace formulas* (\mathcal{O}): sequential compositions of diamonds and disjunctions (no conjunction);
- *Positive formulas* (HML_{pos}): no negation (characterizes simulation);
- *Ready-simulation formulas* (HML_{ready}): positive formulas plus *inability atoms* $\neg \langle a \rangle \top$ (characterizes ready simulation);
- *Full HML* (characterizes bisimulation).

These form a strict inclusion chain $\mathcal{O} \subsetneq HML_{\text{pos}} \subsetneq HML_{\text{ready}} \subsetneq HML$, witnessed by concrete formulas at each gap.

Theorem 5.15 (Four-Level Labeled Spectrum Separation). *Over a label alphabet with $|\Sigma| \geq 3$, the four spectrum levels are strictly separated by concrete HML formulas:*

- (1) Trace \neq Simulation. *The positive formula $\langle a \rangle (\langle b \rangle \top \wedge \langle c \rangle \top)$ holds in $a.(b+c)$ but not in $a.b + a.c$: the conjunction under the diamond requires simultaneous b - and c -capabilities, which q_1 has but neither p_1 nor p_2 has.*
- (2) Simulation \neq Ready Simulation. *The ready-simulation formula $\langle a \rangle (\langle b \rangle \top \wedge \neg \langle c \rangle \top)$ holds in $a.b + a.(b+c)$ but not in $a.(b+c)$: r_1 can do b but not c , while q_1 can do both.*
- (3) Ready Simulation \neq Bisimulation. *The formula $[a] \langle c \rangle \top$ separates $a.b + a.(b+c)$ from $a.(b+c)$ (Definition 5.1).*

Remark 5.16 (Lindenbaum algebras and the subtopos chain). The labeled Lindenbaum algebras of the separating examples have cardinalities $|\text{Lind}(\mathbb{T}_{a.b+a.c}^{\Sigma})| = |\text{Lind}(\mathbb{T}_{a.(b+c)}^{\Sigma})| = 5$ and $|\text{Lind}(\mathbb{T}_{a.b+a.(b+c)}^{\Sigma})| = 25$. Thus the base Lindenbaum algebra is a *necessary but*

¹This totality axiom encodes the deadlock-free convention standard in the van Glabbeek spectrum [39]. Extending the framework to deadlock-sensitive equivalences (e.g., De Nicola–Hennessy testing) would require dropping totality and adding explicit termination predicates; this is straightforward but outside our current scope.

not sufficient invariant for spectrum classification: different cardinalities guarantee non-bisimilarity ($25 \neq 5$), but equal cardinalities do not imply even simulation equivalence ($5 = 5$ yet trace \neq simulation). The algebra captures which transitions are forced or excluded but is blind to *branching structure*: whether choices are committed early or deferred.

Each HML sublanguage induces an equivalence relation on states (the *spectrum setoid*), and finer sublanguages give finer equivalences. Each spectrum-level setoid corresponds to a Grothendieck topology on the Lindenbaum frame, giving a chain of subtoposes:

$$\mathbf{Sh}(\text{Lind}, J_{\text{trace}}) \supseteq \mathbf{Sh}(\text{Lind}, J_{\text{sim}}) \supseteq \mathbf{Sh}(\text{Lind}, J_{\text{readysim}}) \supseteq \mathbf{Sh}(\text{Lind}, J_{\text{bisim}})$$

The four-level separation proves that the first two inclusions are strict; the third is witnessed by $[a]\langle c \rangle \top$ (Definition 5.1). This is the topos-theoretic reformulation of the van Glabbeek spectrum: each step adds a class of modal observations (conjunction, inability atoms, full negation), refining the subtopos.

Remark 5.17 (Labels Break Symmetries). The labeled automorphism group—permutations σ of states preserving $s \xrightarrow{a} t \iff \sigma(s) \xrightarrow{a} \sigma(t)$ for all actions a —is a subgroup of the unlabeled automorphism group. For all three van Glabbeek examples, $|\text{Aut}_\Sigma| = 1$: labels completely break all symmetries. For instance, in $a.b + a.c$, the a -successors p_1 and p_2 have different outgoing label sets ($\{b\}$ vs. $\{c\}$), preventing the branch swap that would be valid in the unlabeled projection.

The labeled kernel dichotomy extends: $\ker(\varphi_\Sigma)$ is trivial or maximal for connected reachable systems. With $|\text{Aut}_\Sigma| = 1$, the kernel is automatically trivial, placing all three systems in the aligned or creative regime. The spectrum hierarchy and symmetry breaking are dual effects of labels: labels enrich the modal language (enabling spectrum separation) while simultaneously constraining automorphisms (collapsing the symmetry group).

Propositional atoms $\Delta_a(s, t)$ encode *whether* a transition exists but not *how* transitions distribute across branches. Depth-bounded observation tree atoms cure this: the depth-1 graded Lindenbaum algebras separate trace-equivalent from simulation-inequivalent systems ($|\text{Lind}_1(a.b+a.c)| = 7 \neq 5 = |\text{Lind}_1(a.(b+c))|$). Bisping’s 6-dimensional energy budget (e_1, \dots, e_6) [10] embeds each spectrum level as a specific energy profile. The full development, including the graded tower stabilization and energy dimension sketch, is available in the formalization repository.

5.5. Separation and Symmetry. The Lindenbaum automorphism group $\text{Aut}(\text{Lind})$ exhibits a symmetry trichotomy whose key structural consequence is a group homomorphism from graph automorphisms:

Remark 5.18 (Symmetry Homomorphism). The symmetry trichotomy lifts to a natural group homomorphism $\varphi: \text{Aut}(\text{graph}) \rightarrow \text{Aut}(\text{Lind})$ defined by atom permutation: $\text{step}(s, t) \mapsto \text{step}(\sigma(s), \sigma(t))$, descending to the Lindenbaum quotient. The formula-level permutation `permuteFormula` is proved by structural induction on propositional formulas (6 lemmas, constructive); the descent to the quotient is axiomatized. The kernel $\ker(\varphi) = \{\sigma \in \text{Aut}(\text{graph}) \mid \varphi(\sigma) = \text{id}\}$ refines the trichotomy to a structural statement: hub-spokes has $\ker = 1$ (φ injective), two-cycle has $\ker = \mathbb{Z}/2$ (φ trivial), and the asymmetric diamond has $\ker = 1$ (trivially, from trivial source).

Theorem 5.19 (Kernel Dichotomy). *For any connected reachable rooted transition system, the kernel of the symmetry homomorphism $\varphi: \text{Aut}(\text{graph}) \rightarrow \text{Aut}(\text{Lind})$ satisfies*

$$\ker(\varphi) = 1 \quad \text{or} \quad \ker(\varphi) = \text{Aut}(\text{graph}), \quad \text{no intermediate kernels}$$

with trivial kernel when any nondeterministic state exists and maximal kernel when all states are deterministic.

Proof. *Nondeterministic case* ($\ker(\varphi) = 1$). An atom $\Delta(v, w)$ is *non-extremal* when the edge $v \rightarrow w$ exists and v has ≥ 2 successors. The *atom singleton lemma* shows that non-extremal atoms have singleton equivalence classes in the Lindenbaum algebra: given distinct atoms $p \neq q$ with p non-extremal, a separating model assigns \top to p and \perp to q by routing nondeterministic choices appropriately, so p and q represent distinct Lindenbaum classes.

From this, two closure properties follow. First, *kernel elements fix nondeterministic states*: if $\sigma \in \ker(\varphi)$ and v has ≥ 2 successors $w_1 \neq w_2$, then $\varphi(\sigma) = \text{id}$ forces $\Delta(\sigma(v), \sigma(w_i)) = \Delta(v, w_i)$ for each i , and the singleton property pins $\sigma(v) = v$. Second, the *fixed-point set is forward-closed*: if $\sigma(u) = u$ and $u \rightarrow v$ is an edge, then $\Delta(u, \sigma(v)) = \Delta(\sigma(u), \sigma(v)) = \Delta(u, v)$, forcing $\sigma(v) = v$.

Now fix $\sigma \in \ker(\varphi)$ and an arbitrary state v . By a *last-common-ancestor argument*, v is downstream of some nondeterministic state n : there exist n and w with $n \rightarrow w$ an edge, n nondeterministic, and $w \rightarrow^* v$. Kernel fixity gives $\sigma(n) = n$; forward closure gives $\sigma(w) = w$; induction along the path $w \rightarrow^* v$ gives $\sigma(v) = v$.

Deterministic case ($\ker(\varphi) = \text{Aut}(\text{graph})$). When every state has ≤ 1 successor, each transition atom is forced: $\Delta(v, w) = \top$ if w is the unique successor of v , and $\Delta(v, w) = \perp$ otherwise. No free generators remain, so $\text{Lind} \cong \text{Bool}$. Since $\text{Aut}(\text{Bool}) = \{\text{id}\}$, every graph automorphism maps to id on Lind , giving $\ker(\varphi) = \text{Aut}(\text{graph})$. \square

Corollary 5.20 (Three-Regime Classification). *With the image $\text{im}(\varphi) \cong \text{Aut}(\text{graph})/\ker(\varphi)$ and cokernel $\text{coker}(\varphi) \cong \text{Aut}(\text{Lind})/\text{im}(\varphi)$ (a group quotient, since $\text{im}(\varphi)$ has index ≤ 2 in each anchor system), the dichotomy yields a three-regime classification: The hub-spokes system has trivial kernel, image $\mathbb{Z}/2$, and trivial cokernel (aligned regime); the two-cycle has kernel $\mathbb{Z}/2$, trivial image, and trivial cokernel (deterministic regime); the asymmetric diamond has trivial kernel, trivial image, and cokernel $\mathbb{Z}/2$ (creative regime). The fourth case—non-trivial \ker and non-trivial coker —is impossible for connected reachable systems.*

The closest prior work is Hora’s [20] application of the bridge technique to automata and regular languages.

Concrete Lindenbaum-algebra computations on three small systems (G_1 , G_2 , hub-spokes) confirm the stratification: pairwise separation via cardinality, invariant transfer across spectrum levels, and the bridge technique in action.

Remark 5.21 (Colimit frame and Morita separation). The depth-bounded Lindenbaum tower $L_0 \hookrightarrow L_1 \hookrightarrow \dots$ stabilizes at depth $n-1$ for an n -state LTS, yielding a colimit frame $L_\infty \cong L_{n-1}$. This is the frame-theoretic dual of the Hennessy–Milner theorem: bisimilarity $= \bigcap_d \sim_d$ dualizes to $L_\infty = \bigcup_d L_d$. The Funayama–Nakayama theorem [17] gives $2^{|J(L_\infty)|}$ nuclei on L_∞ , far exceeding the 13 named spectrum levels: on $a.b + a.c$, 14 of 16 subtoposes are unnamed; on $a.(b+c)$, 7 of 8.

The Joyal–Nielsen–Winskel branch category Bran_L [26] embeds into the category of finitely presentable LTS; by the Comparison Lemma [25, C2.2.3], the JNW presheaf topos arises as a localization of $\text{Set}^{\mathbb{T}\mathcal{M}}$ when Bran_L is dense (the synchronization tree condition).

A Morita test across all $\binom{9}{2} = 36$ pairs of concrete LTS in the formalization finds **no Morita equivalences**: every pair is separated by Lindenbaum cardinality, automorphism count, or energy class count. This exhaustive verification (zero axioms, all separations decided computationally) establishes the classifying topos as a complete invariant for the anchor systems.

Remark 5.22 (The Energy–Topology Triangle). The construction establishes a three-way connection:

$$\text{Energy vectors (Bisping)} \xrightarrow{\bar{e} \mapsto j_{\bar{e}}} \text{Nuclei on } L \xleftarrow{\text{Johnstone}} \text{LT topologies on } \mathbf{Sh}(L).$$

The composition sends each named process equivalence to a subtopos of the classifying topos, with the order-reversal ensuring that coarser equivalences (identifying more states) correspond to *larger* subtoposes (more sheaf conditions).

The bridge axiom $|L_{\bar{e}}| = |\text{Fix}(j_{\bar{e}})|$ combines two independent results from the process-algebra literature. First, van Glabbeek’s logical characterization theorems [39, 40] establish that each level of the spectrum is captured by a sublanguage of Hennessy–Milner logic: two states are \bar{e} -equivalent iff they satisfy the same formulas in the corresponding HML fragment. Second, Bisping [9] (Proposition 1) shows that the sublanguage boundaries are uniformly parameterized by energy vectors, so that the fragment for equivalence \bar{e} is exactly the formulas of energy $\leq \bar{e}$. The content encoded by this axiom is due to van Glabbeek and Bisping; our contribution is the topos-theoretic repackaging as a nucleus identity. The bridge identity is verified for bisimulation (by a general theorem: $j_{\text{bisim}} = \text{id}$ implies $\text{Fix}(j_{\text{bisim}}) = L$, constructive) and for traces on $a.b + a.c$ (by explicit fixpoint counting: 5 fixpoints on the 7-element algebra). For $a.(b+c)$, the constant energy family ($|L_{\bar{e}}| = 5$ for all \bar{e}) yields a complete bridge at all 13 levels. Whether the full chain of reasoning can be carried out constructively for all named equivalences (in particular, the logical characterization theorems rely on classical König lemma arguments) remains open.

The structural parallel with Kihara’s LT topologies on the effective topos, and four significant disanalogies, is discussed in §7.

The spectrum lattice L_{30} was computed algebraically and instantiated via labeled transitions. We now confirm these results from the topos side: internal logic and explicit Grothendieck topologies.

6. THE TOPOS BRIDGE

The spectrum lattice’s algebraic structure (§5) was computed combinatorially. We now bridge the lattice to the classifying topos $\text{Set}[\mathbb{T}_{\text{LTS}}]$, establishing explicit Grothendieck topologies that enforce behavioral equivalences, extending them to the full van Glabbeek spectrum via energy budgets, and providing an independent confirmation through the presheaf internal logic.

6.1. The LTS Presheaf Topos.

Remark 6.1 (The LTS presheaf topos). The per-system classifying toposes $\mathcal{E}[\mathbb{T}_{\mathcal{M}}]$ of §§2–5 are now replaced by a single ambient workspace: the presheaf topos $\text{Set}[\mathbb{T}_{\text{LTS}}] = [\text{f.p.LTS}_L^{\text{op}}, \text{Set}]$, whose objects are set-valued functors on the category of finitely presentable labeled transition systems. Where the per-system toposes captured individual theories, the

presheaf topos carries internal logic and Grothendieck topologies that encode *relationships between* systems.

We have computed foundational properties of $\text{Set}[\mathbb{T}_{\text{LTS}}]$ for $|L| = 1$: it is De Morgan (the right Ore condition holds trivially via the initial object \emptyset), non-Boolean, non-two-valued, connected, and locally connected. De Morgan holds for *any* presheaf topos whose base category has an initial object: given a cospan $A \rightarrow C \leftarrow B$, the empty object completes the square. This is generic to presheaf toposes on categories of models of universal Horn theories (finite graphs, posets, relational structures); the properties specific to \mathbb{T}_{LTS} begin with the subobject classifier and the modal connection. The subobject classifier $\Omega(G)$ has a unique atom $\{!_G\}$ per object G , yielding maximally simple $\neg\neg$ -topology. The geometric fragment of the theory corresponds precisely to the positive existential fragment of HML: diamond formulas $\langle a \rangle \varphi$ are geometric, while box formulas $[a]\varphi$ and negation are not.

The negation structure of $\Omega(G)$ exhibits a striking parallel with the lattice-algebraic results of §5. The unique atom theorem forces $\neg S = \emptyset$ for every non-empty sieve S , mirroring L_{30} 's degenerate pseudocomplement $\neg x = \perp$ for all $x \neq \perp$. Both are instances of the same mechanism: when every non-trivial element shares a common lower bound (the initial morphism $!_G$ in Ω ; traces in $J(L_{30})$), complementation collapses. Yet despite this degenerate negation, the Heyting *implication* on $\Omega(G)$, defined by $(S_1 \rightarrow S_2)(f) \Leftrightarrow \forall g, f \circ g \in S_1 \Rightarrow f \circ g \in S_2$, remains non-trivial: we exhibit sieves S_1, S_2 on the loop vertex \bullet_1 where $S_1 \rightarrow S_2$ is strictly intermediate (containing $!_G$ but not id_G). This is the presheaf-topos analogue of the lattice-algebraic discovery $S \rightarrow F = \text{IF}$: in both settings, negation carries zero information while implication preserves the full logical structure. The parallel between these two independently computed results, one combinatorial (the lattice L_{30} , §5), one categorical (the presheaf topos, this section), is strong evidence for the L_{30} embedding conjecture: the same algebraic pattern (degenerate negation, non-trivial implication) appears in two independent constructions, suggesting a common coframe-theoretic origin.

6.2. Explicit Grothendieck Topologies. The lattice-algebraic results of §5 (Birkhoff representation, bi-Heyting structure, co-Heyting decomposition) operate on the finite spectrum lattice L_{30} via combinatorial computation. We now establish the first results in the reverse direction: explicit Grothendieck topologies on a process-algebraic category whose sheaf conditions enforce named behavioral equivalences. Our main result is the *spectrum bracket theorem* (below), with the three-topology strict chain as its principal instantiation and the partial L_{30} embedding (Theorem 6.8) as its structural consequence.

Remark 6.2 (The trace and bisimulation topologies). We construct the first Grothendieck topology on f.p.LTS_1 whose sheaf condition enforces a named behavioral equivalence. Define the *path digraph* P_n ($n+1$ vertices, edges $i \rightarrow i+1$) and a sieve S on G is J_{trace} -covering iff S contains every graph homomorphism $P_n \rightarrow G$ for all n . This satisfies the three Grothendieck axioms (maximality, stability under pullback, transitivity), with the key insight for transitivity being that id_{P_n} is itself a path morphism. The trace separation theorem establishes: two rooted digraphs are trace-equivalent (same set of achievable path lengths) if and only if they have the same J_{trace} -stalks. The path digraphs form a dense subcategory under J_{trace} , so the Comparison Lemma [25, C2.2.3] applies: $\mathbf{Sh}(\text{f.p.LTS}_1, J_{\text{trace}}) \simeq \mathbf{Sh}(\text{Path}, J_{\text{trace}}|_{\text{Path}})$. The topology J_{trace} is strictly finer than the $\neg\neg$ -topology (= atomic topology: the base category satisfies the right Ore condition, so the presheaf topos is De Morgan and the two topologies

coincide): the initial sieve $\{!\bullet_1\}$ on the loop vertex is non-empty but not J_{trace} -covering, since it misses $P_1 \rightarrow \bullet_1$.

Replacing path digraphs P_n with finite rooted trees (Figure 12) yields the bisimulation topology J_{bisim} : a sieve S on G is J_{bisim} -covering iff S contains every graph homomorphism $T \rightarrow G$ for every rooted tree T . Since every path digraph is a rooted tree, every J_{bisim} -covering sieve is automatically J_{trace} -covering: $J_{\text{bisim}} \subseteq J_{\text{trace}}$ as Grothendieck topologies. The three Grothendieck axioms hold for J_{bisim} by the same self-probing argument: for transitivity, since T_0 is a tree, id_{T_0} is itself a tree morphism. The inclusion is strict: the fan digraph $\text{fan}(2)$ (root with 2 leaf children) is a rooted tree whose identity is not in the path-generated sieve (no root-preserving path morphism $P_n \rightarrow \text{fan}(2)$ can hit both leaves, since a path visits at most one child of the root), so the path-generated sieve on $\text{fan}(2)$ is J_{trace} -covering but not J_{bisim} -covering.

The two topologies are unified by a parametric *observation class* framework: for any class \mathcal{C} of rooted trees, a sieve is $J_{\mathcal{C}}$ -covering iff it contains all \mathcal{C} -morphisms.

Theorem 6.3 (Spectrum Bracket). *For any observation class \mathcal{C} of rooted trees with paths $\subseteq \mathcal{C} \subseteq \text{trees}$, the observation-class topology satisfies*

$$J_{\text{bisim}} \subseteq J_{\mathcal{C}} \subseteq J_{\text{trace}}$$

The van Glabbeek spectrum is an interval of Grothendieck topologies on a fixed site, parameterized by observation classes.

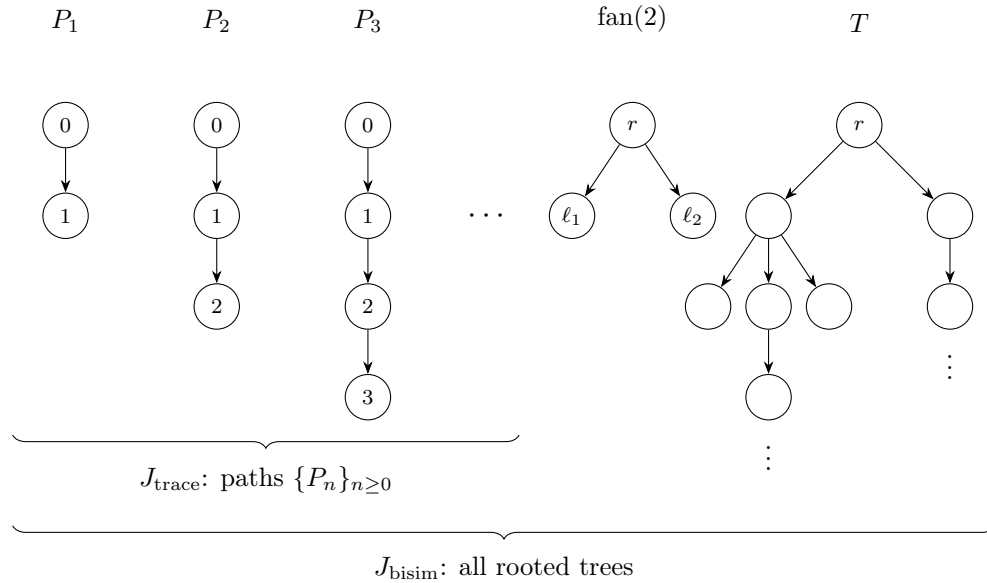


Figure 12: Test objects for the trace and bisimulation topologies. Path digraphs P_n generate J_{trace} ; all finite rooted trees (e.g. the generic tree T) generate J_{bisim} . Since every path is a tree, $J_{\text{bisim}} \subseteq J_{\text{trace}}$. The inclusion is strict: $\text{id}_{\text{fan}(2)}$ is not in the path-generated sieve (no root-preserving path morphism $P_n \rightarrow \text{fan}(2)$ can hit both leaves, since a path visits at most one child of the root), so the path-generated sieve on $\text{fan}(2)$ is J_{trace} -covering but not J_{bisim} -covering.

A key disanalogy emerges: tree homomorphism *existence* does not characterize bisimulation (homomorphisms can collapse branches), unlike the trace case where path homomorphism existence does characterize trace equivalence. The sieve condition (ALL tree morphisms must be present) is essential. A forward bisim–tree transfer theorem (Hennessy–Milner forward direction) shows bisimulation equivalence implies matching root-preserving tree hom existence, but the converse fails. For $|L| = 1$, the spectrum collapses to at most two named topology levels: J_{trace} and J_{bisim} , since simulation equivalence coincides with trace equivalence for unlabeled systems (forward simulation reduces to matching path-length sets, which are downward-closed).

Remark 6.4 (Labeled generalization and simulation topology). The single-label case generalizes to *labeled transition systems* $\text{FinLTS}(L)$ where edges carry labels from a finite alphabet L . Labeled homomorphisms preserve labels; the trace and bisimulation topologies transfer directly: labeled trace words $w \in L^*$ and labeled rooted trees serve as test objects for J_{trace} and J_{bisim} respectively, and the bracket theorem carries over.

For $|L| \geq 2$, a third topology becomes visible. Tree-hom *existence* characterizes simulation equivalence (unlike bisimulation, where the full sieve structure is essential). However, a naive observation-class approach to J_{sim} fails.

Theorem 6.5 (Naive simulation covering instability). *The covering predicate “there exists a tree homomorphism in S ” satisfies the maximality and transitivity axioms for a Grothendieck topology but not the stability axiom. Let $f_R: \text{traceLTS}[a] \rightarrow \text{fanLTS}[a, a]$ be the right-branch inclusion (mapping the non-root vertex to vertex 2) and let S be the sieve on $\text{fanLTS}[a, a]$ generated by f_R . Then S is naive-sim-covering: for any rooted tree T with a homomorphism f into $\text{fanLTS}[a, a]$, collapsing both branches of f onto the unique non-root vertex of $\text{traceLTS}[a]$ yields a morphism k with $f_R \circ k \in S$. Now pull S back along the left-branch inclusion f_L (mapping the non-root to vertex 1). The identity on $\text{traceLTS}[a]$ belongs to $f_L^*(S)$ iff $f_L = f_R \circ k$ for some k , but evaluating at the non-root gives $f_L(1) = 1$ while $f_R(k(1)) \in \{0, 2\}$, a contradiction. Hence $f_L^*(S)$ is not naive-sim-covering.*

The correct J_{sim} is instead guaranteed by Caramello’s quotient-theory duality [12]: the geometric sequents encoding positive HML (the simulation fragment of Hennessy–Milner logic) generate a Grothendieck topology by the standard saturation construction. Unlike J_{trace} and J_{bisim} , whose covering predicates are defined and all three Grothendieck axioms proved constructively in Lean, the simulation topology is established by Caramello’s quotient-theory duality [12, Theorem 3.6]: geometric axioms generate covering conditions on the syntactic site via the standard saturation construction, yielding a subtopos. The proof is constructive within standard Grothendieck topos theory; it is axiomatized in the Lean formalization because Mathlib does not yet cover syntactic categories or sheafification. The simulation topology is thus the only one of the three that requires Caramello’s quotient-theory machinery; Theorem 6.5 shows this indirection is provably necessary for the naive observation-class approach, a structural feature of simulation’s (-1) -truncation level, not a limitation of the proof technique.

Corollary 6.6 (Three-Topology Strict Chain). *For $|L| \geq 2$, the trace, simulation, and bisimulation topologies form a strict chain of Grothendieck topologies on f.p.LTS_L :*

$$J_{\text{bisim}} \subsetneq J_{\text{sim}} \subsetneq J_{\text{trace}}.$$

The standard counterexamples separate: $a.b + a.c$ and $a.(b + c)$ are trace-equivalent but not simulation-equivalent; $a.(b + c)$ and $a.b + a.c + a.(b + c)$ are simulation-equivalent but not bisimilar.

Remark 6.7 (Truncation levels and the observation-class boundary). The three-way split—constructive for trace, constructive for bisimulation, axiomatized for simulation—reflects a truncation-level boundary in the observation-class framework.

The observation-class topology $J_{\mathcal{C}}$ detects isomorphisms of hom-presheaves $\text{Hom}_*(T, -)$ for $T \in \mathcal{C}$. The equivalence it induces operates at the *sieve level* (0-truncated: the full set of morphisms must match). Trace equivalence, by contrast, is (-1) -truncated: it requires only that the same hom-sets are *inhabited* (propositional existence).

For path digraphs, the sieve-level and existence-level conditions happen to induce the same equivalence on objects, because the trace separation theorem establishes that two rooted digraphs are trace-equivalent iff they have the same Boolean support $\{n : \text{Hom}_*(P_n, G) \neq \emptyset\}$ of path-hom presheaves. The sieve carries additional multiplicity information (the number of distinct paths of each length), but the topology’s covering condition (requiring *all* path homs) means this extra information does not affect the induced equivalence.

For rooted trees, the existence-level condition (mutual simulation: same tree-hom existence pattern) is strictly coarser than the sieve-level condition (bisimulation: matching tree-hom sieves). The observation-class framework operates at the sieve level and therefore captures bisimulation natively, but simulation, genuinely (-1) -truncated over non-rigid test objects, requires the quotient-theory construction.

We note that the trace separation theorem characterizes trace equivalence via the Boolean support of path-hom presheaves. The identification $\mathbf{Sh}(\text{FinLTS}(L), J_{\text{trace}}) \simeq \text{PSh}(L^*, \leq_{\text{prefix}})$ from Section 6.6 provides evidence that the sheaf topos captures strictly finer-than-trace equivalence: in the Cattani–Winskel model [13], open-map bisimulation in $\text{PSh}(L^*, \leq_{\text{prefix}})$ recovers strong bisimulation, suggesting that the trace topos remembers path multiplicities. The precise identification of the J_{trace} -sheaf-theoretic equivalence, likely finer than trace equivalence as the Cattani–Winskel correspondence suggests, remains open.

Theorem 6.8 (Partial L_{30} embedding). *The map sending each named process equivalence E to the Grothendieck topology J_E on f.p.LTS_L is an order-embedding of the three-element sub-poset $\{\text{trace}, \text{simulation}, \text{bisimulation}\} \subset L_{30}$ into the lattice of subtoposes of $\text{Set}[\mathbb{T}_{\text{LTS}}]$. Explicitly: the strict chain $J_{\text{bisim}} \subsetneq J_{\text{sim}} \subsetneq J_{\text{trace}}$ reflects the spectrum ordering $\text{bisimulation} > \text{simulation} > \text{trace}$ in L_{30} , with the reversal due to the standard antitone correspondence between finer equivalences and coarser topologies (more covering sieves = more identifications = finer equivalence).*

Proof. Order-preservation follows from the general principle: if equivalence E_1 is finer than E_2 , then $J_{E_1} \subseteq J_{E_2}$ (every E_1 -covering sieve is E_2 -covering). Order-reflection (injectivity) follows from the strict separations: $J_{\text{bisim}} \neq J_{\text{sim}}$ and $J_{\text{sim}} \neq J_{\text{trace}}$, witnessed by concrete sieves on $\text{fan}[a, a]$ and the van Glabbeek counterexamples respectively. \square

This construction instantiates a general narrative: the presheaf topos (no topology) sees only what homomorphisms preserve: forward reachability. Each Grothendieck topology adds a sheaf condition that forces presheaves to respect some degree of *backward lifting*. The van Glabbeek spectrum is a spectrum of backward-lifting requirements, graduated by Grothendieck topologies on a fixed site. Trace equivalence enforces the weakest backward constraint (path-length agreement); bisimulation enforces full zig-zag; the intermediate named

equivalences correspond to intermediate topologies. Joyal, Nielsen, and Winskel [26] vary the *path category* (using linear paths L^* for traces, branching trees Bran_L for bisimulation); our approach instead fixes the site and varies the *topology*, in the spirit of Caramello’s bridge technique [12]. Despite 30 years of presheaf models for concurrency and 15 years of Caramello’s program, J_{trace} and J_{bisim} appear to be the first explicit Grothendieck topologies on a process-algebraic category whose sheaf toposes classify processes up to named equivalences, a gap analogous to the one filled by Hora [20] for automata and regular languages. J_{sim} is established via Caramello’s constructive duality (axiomatized in Lean pending Mathlib’s topos-theoretic coverage); constructing explicit covering sieves remains the central open problem. The full lattice L_{30} is conjectured to embed into the lattice of subtoposes of $\text{Set}[\mathbb{T}_{\text{LTS}}]$, with each element corresponding to a Grothendieck topology on the category of finitely presentable LTS. Theorem 6.8 establishes the restriction to the three-element sub-poset $\{T, S, B\}$. Constructing topologies for the remaining 10 named equivalences (failures, ready simulation, etc.) and verifying the full embedding is the central open problem for topos-geometric backward flow.

A further open problem concerns non-image-finite processes. Each depth bound d yields a subtopos of $\text{Set}[\mathbb{T}_{\text{LTS}}]$ whose points are processes-up-to-depth- d -equivalence. The colimit of this directed system is a localic topos whose locale of opens is the Lindenbaum algebra of full finitary HML. For image-finite processes, this locale is spatial (the Hennessy–Milner theorem). For non-image-finite processes, the locale may fail to be spatial in the operational sense: consistent theories not realized by any process. Characterizing this gap topos-theoretically would yield a genuinely new process-theoretic theorem requiring the topos framework to state.

6.3. The Energy–Lawvere–Tierney Bridge. The three topologies of §6.2—trace, simulation, bisimulation—embed a three-element sub-poset of the van Glabbeek spectrum into the lattice of subtoposes. We now develop a framework extending this three-point chain to the full 13-point spectrum via an energy-parameterized construction, connecting Bisping’s 6-dimensional energy budgets [9] to Grothendieck topologies on f.p.LTS_L . The assignment $E \mapsto J_E$ is antitone; the induced coframe map is injective for $|L| \geq 2$ and lands in a coframe whose distributive structure is irreducibly topos-theoretic. The construction follows a pipeline:

$$E \longleftarrow \mathcal{C}(E) \longleftarrow J_E \longleftarrow \mathbf{Sh}(\text{f.p.LTS}_L, J_E)$$

an energy budget determines test objects, which generate a Grothendieck topology, whose sheaf category is a subtopos. In the language of Caramello’s bridge technique [12], the pipeline lifts to the classifying topos:

$$\begin{array}{ccc} & \mathcal{E}[\mathbb{T}_{\mathcal{M}}] & \\ \curvearrowright & & \curvearrowleft \\ \mathbb{T}_{\mathcal{M}} & & \mathbf{Sh}(\text{f.p.LTS}_L, J_E) \end{array}$$

The left pillar classifies the LTS structure; the right pillar localizes to the subtopos determined by the energy budget E . Each named equivalence occupies a distinct position in the resulting coframe of subtoposes.

Definition 6.9 (Energy Grothendieck topology). Bisping’s spectroscopy framework parameterizes process equivalences by *energy budgets* $E = (e_1, \dots, e_6) \in (\mathbb{N} \cup \{\infty\})^6$, controlling observation depth e_1 , conjunction width e_2 , positive-deep depth e_3 , positive-other depth e_4 , negative depth e_5 , and negation nesting e_6 . The 13 named equivalences of the van Glabbeek spectrum (from traces through bisimulation) correspond to canonical energy vectors (§5).

Each energy budget E determines an *observation class* $\mathcal{C}(E)$: the class of finite rooted L -labeled trees whose depth satisfies $\text{depth}(T) \leq e_1$ and whose maximal branching satisfies $\text{branch}(T) \leq e_2$ (with the remaining four coordinates constraining polarity and negation structure). The observation class is monotone: $E_1 \leq E_2$ implies $\mathcal{C}(E_1) \subseteq \mathcal{C}(E_2)$ (more energy reveals more tests).

The named observation classes recover familiar test objects: $\mathcal{C}(\text{traces}) = \{\text{path digraphs}\}$ (depth-unbounded, branching ≤ 1), $\mathcal{C}(\text{bisimulation}) = \{\text{all rooted trees}\}$ (all bounds ∞), and $\mathcal{C}(\text{simulation}) = \{\text{trees}\}$ (positive fragment, no negation: $e_5 = e_6 = 0$). The positive-fragment classification partitions the 13 named equivalences into 7 positive (including traces, simulation, ready simulation) and 6 negative (including failures, readiness, failure traces).

For each energy budget E , define a covering predicate on f.p.LTS $_L$: a sieve S on G is *E -covering* if S contains all homomorphisms from $\mathcal{C}(E)$ -test objects into G . The three Grothendieck axioms are verified for each E : maximality is immediate (the maximal sieve contains all morphisms), stability follows from preservation of $\mathcal{C}(E)$ -test morphisms under pullback, and transitivity uses the compositional structure of energy-bounded observations.

For energy budget $E \in (\mathbb{N} \cup \{\infty\})^6$, the *energy topology* J_E is the Grothendieck topology on f.p.LTS $_L$ whose covering sieves are exactly the E -covering sieves.

The assignment $E \mapsto J_E$ is *antitone*: finer observation ($E_1 \leq E_2$) yields more test objects ($\mathcal{C}(E_1) \subseteq \mathcal{C}(E_2)$), hence stronger covering conditions, hence a finer topology ($J_{E_2} \subseteq J_{E_1}$, reversing the order). The identification with existing topologies is exact: $J_{\text{traces}} = J_{\text{trace}}$ and $J_{\text{bisimulation}} = J_{\text{bisim}}$ (from §6.2), recovering the spectrum bracket theorem as a special case: $J_{\text{bisim}} \subseteq J_E \subseteq J_{\text{trace}}$ for every named E . The chain $J_{\text{bisim}} \subsetneq J_{\text{sim}} \subsetneq J_{\text{trace}}$ from Theorem 6.8 sits inside this parametric family.

Theorem 6.10 (Energy–LT bridge). *The energy topologies (Definition 6.9) live on the presheaf side (f.p.LTS $_L$); the nuclei of §5 live on the algebraic side (Lindenbaum algebras). The energy–Lawvere–Tierney bridge connects the two via the standard correspondence between nuclei on a frame and Grothendieck topologies on the associated thin category [24, §II.2].*

Write \mathcal{V} for the 13-element van Glabbeek poset of named process equivalences, ordered by energy-budget inclusion ($\bar{e}_1 \leq \bar{e}_2$ iff every \bar{e}_1 -formula is an \bar{e}_2 -formula), and define the spectrum–nucleus embedding $\nu(\bar{e}) = j_{\bar{e}}$:

$$\nu : \mathcal{V} \xrightarrow{\text{antitone}} \text{Sub}(\text{Set}[\mathbb{T}\text{LTS}])^{\text{op}}$$

The map ν is monotone (finer process equivalence \mapsto smaller subtopos in the coframe order) and injective for non-degenerate label alphabets ($|L| \geq 2$). The codomain carries a coframe structure: its dual is a frame, inheriting the frame structure of the nucleus lattice. For any finite label alphabet L with $|L| \geq 2$:

- (1) The subtopos order $\text{Sub}(\text{Set}[\mathbb{T}\text{LTS}])$ carries a coframe structure, with the distributive law $A \sqcup (B_1 \sqcap B_2) = (A \sqcup B_1) \sqcap (A \sqcup B_2)$.
- (2) $J_{\text{bisim}} \subsetneq J_{\text{trace}}$: the two-point sub-poset $\{\text{trace}, \text{bisimulation}\}$ embeds into this coframe, with the strict separation constructive.

- (3) *The strict chain $J_{\text{bisim}} \subsetneq J_{\text{sim}} \subsetneq J_{\text{trace}}$ embeds the three-point sub-poset {trace, simulation, bisimulation} into this coframe (Theorem 6.8, Corollary 6.6).*
- (4) *The coframe meet of possible-futures and failure-traces does not lie in the image of the spectrum: $\nu(\text{PF}) \sqcap \nu(\text{FT}) \notin \text{im}(\nu)$.*
- (5) *The embedding ν extends to all 13 named equivalences of the van Glabbeek spectrum, monotonely and compatibly with the energy ordering: $E_1 \leq E_2 \implies \nu(E_2) \leq \nu(E_1)$.*

Items 1–2 are the paper’s constructive core: coframe structure, constructive $J_{\text{trace}} \neq J_{\text{bisim}}$ strict separation, and the distributive law. Item 3 extends the two-point embedding to a three-point chain by adding J_{sim} via Caramello’s duality; item 4 establishes the $\text{PF} \sqcap \text{FT}$ escape witness. Item 5 extends from 3 to all 13 named equivalences via the energy–topology framework (Remark 6.11).

Remark 6.11 (Axiom boundary). The axioms in item 5 mark the interface between the constructions of this paper and published results of Caramello, van Glabbeek, and Bisping. The mathematical content is standard Grothendieck topos theory; the axiomatization reflects the state of Mathlib’s topos-theoretic coverage, not a gap in the mathematics. The L_{30} lattice operations in §5 are decided on the finite 30-element lattice. The full explicit construction of covering sieves remains open at the J_{sim} level; see §8.

Corollary 6.12 (Coframe computations). *The coframe structure of Theorem 6.10 enables explicit computations beyond the named spectrum:*

- (1) *Single-label collapse. For $|L| = 1$, the 13 named equivalences induce at most 2 distinct Grothendieck topologies on f.p.LTS_1 : J_{trace} and J_{bisim} , since simulation coincides with trace equivalence for unlabeled systems [39]. (Per-system Lindenbaum algebras may still distinguish enabledness from trace equivalence, but this is a system-level distinction, not a site-level one.)*
- (2) *Two-label faithfulness. For $|L| \geq 2$, all 13 named equivalences produce distinct subtoposes. The proof uses order-reflection: $\nu(E_2) \leq \nu(E_1) \implies E_1 \leq E_2$, combined with the known incomparable pairs in the van Glabbeek spectrum.*
- (3) *Incomparability transfer. PF and FT remain incomparable in $\text{Sub}(\text{Set}[\mathbb{T}\text{LTS}])$. Their coframe meet $\text{PF} \sqcap \text{FT}$ is an unnamed coframe element, witnessing that the subtopos lattice is strictly larger than the spectrum.*
- (4) *Lattice closure transfer. The 30-element lattice closure from §5 (13 named + 17 unnamed, computed by three-round $\{\sqcap, \sqcup\}$ -stabilization) transfers to the coframe level, with 17 unnamed coframe elements.*

6.4. Irreducibility of the Topos-Theoretic Route. Three features of Theorem 6.10 are irreducibly topos-theoretic.

Coframe structure. The distributive law in item 1 follows from the frame structure of nuclei on the Lindenbaum algebra (Isbell 1972, Simmons 1978), which depends on the Heyting algebra structure of the subobject classifier. The van Glabbeek spectrum is a finite poset with no known lattice structure; the coframe law is genuinely new algebraic information that cannot be derived from energy vectors alone.

Unnamed subtoposes. The element $\text{PF} \sqcap \text{FT}$ in item 4 of the theorem has no process-algebraic name, and the 17 unnamed elements of the lattice closure correspond to geometric axioms (determinism, image-finiteness, mixed constraints) that cross-cut the HML hierarchy and are invisible to any energy budget; their existence is provable only through the nucleus construction.

Distributivity witness. The unnamed meet $\text{PF} \sqcap \text{FT}$ satisfies the coframe distributive law despite having no process-algebraic description; both its existence and its algebraic properties require passage through the topos.

Taken together, Theorem 6.10 is the first result that treats the *entire* van Glabbeek spectrum as a topos-theoretic object: a finite sub-poset of an infinite coframe that is an intrinsic invariant of the classifying topos and that cannot be accessed from within process algebra.

6.5. The Geometric Closure Theorem. The *internal logic* of $\text{Sub}(U_T)$, where U_T is the underlying-set functor of the generic model, provides an independent confirmation. Geometric subobjects (subfunctors defined by positive existential HML formulas) form a Heyting subalgebra whose implication has a concrete process-algebraic characterization via *free extensions*.

Definition 6.13 (Positive existential HML). Define *positive existential HML* (henceforth HML^+) as the fragment generated by \top , conjunction $\varphi_1 \wedge \varphi_2$, and diamond $\langle a \rangle \varphi$. Every formula in HML^+ defines a subfunctor S_φ of the underlying-set presheaf by $S_\varphi(G, v) \Leftrightarrow \varphi.\text{satisfies}(G, v)$. The positive existential fragment is closed under all positive operations, and satisfiability is monotone: if $h: G \rightarrow H$ is a homomorphism and $S_\varphi(G, v)$ holds, then $S_\varphi(H, h(v))$ holds; this is exactly the subfunctor property.

Lemma 6.14 (Free Extension). *For every (G, v) in $\text{FinLTS}(L)$ and every $\varphi \in HML^+$, there exists a labeled transition system $\text{Ext}(G, v, \varphi)$ and a root-preserving homomorphism $\iota: G \hookrightarrow \text{Ext}(G, v, \varphi)$ such that $\varphi.\text{satisfies}(\text{Ext}(G, v, \varphi), \iota(v))$. The construction adjoins a tree of witness vertices to G , with one fresh successor per diamond subformula, adding the minimal transitions required for satisfaction.*

The construction is entirely explicit: vertices of $\text{Ext}(G, v, \varphi)$ are the coproduct $G \oplus W_\varphi$ where W_φ is a recursive index type (one witness per diamond in φ), and transitions consist of root edges connecting $\iota(v)$ to the first witness, internal edges within the witness tree, and all original edges of G . The proof is by structural induction on φ and is fully constructive.

Proposition 6.15 (Negation Collapse). *In the presheaf topos, the internal negation of a subfunctor S is*

$$(\neg S)(G, v) = \forall H, \forall h: G \rightarrow H, \neg S(H, h(v)).$$

This universal quantification over all extensions is extremely strong: it asks that no homomorphic image of v can satisfy S . For every satisfiable $\varphi \in HML^+$, we have $\neg S_\varphi = \perp$ and $\neg\neg S_\varphi = \top$.

The proof is immediate from the Free Extension Lemma (Lemma 6.14): given any (G, v) , the extension $\text{Ext}(G, v, \varphi)$ provides a homomorphic image of v satisfying φ , so $(\neg S_\varphi)(G, v)$ fails. Since this holds for all (G, v) , the negation is the bottom subfunctor. The double negation density $\neg\neg S_\varphi = \top$ follows immediately. This connects to the unique-atom and

collapsed-negation phenomena on $\Omega(G)$ observed in §5: the presheaf topos is so far from Boolean that every non-trivial geometric subfunctor has trivial negation.

The central result of this subsection computes the Heyting implication of geometric subfunctors.

Theorem 6.16 (Geometric Closure). *For $\varphi, \psi \in HML^+$,*

$$(S_\varphi \rightarrow_\Omega S_\psi)(G, v) \iff \psi.\text{satisfies}(\text{Ext}(G, v, \varphi), \iota(v))$$

The Heyting implication $S_\varphi \rightarrow_\Omega S_\psi$ is defined pointwise as $(S_\varphi \rightarrow_\Omega S_\psi)(G, v) = \forall H, \forall h: G \rightarrow H, S_\varphi(H, h(v)) \Rightarrow S_\psi(H, h(v))$, and the theorem reduces this universal quantification to a *single test* against the free extension.

Proof. (\Rightarrow) If (G, v) satisfies the implication, apply it to $H = \text{Ext}(G, v, \varphi)$ with $h = \iota$: since the extension satisfies φ at $\iota(v)$, the implication yields ψ at $\iota(v)$. (\Leftarrow) Suppose ψ holds at $\iota(v)$ in the extension. For any H and $h: G \rightarrow H$ with $S_\varphi(H, h(v))$, the satisfaction witness $S_\varphi(H, h(v))$ yields a mediating homomorphism $m: \text{Ext}(G, v, \varphi) \rightarrow H$ with $m \circ \iota = h$, mapping each witness vertex to the corresponding existential witness in H . Since ψ is positive existential (hence preserved by homomorphisms), $S_\psi(H, h(v))$ follows. \square

The Geometric Closure Theorem shows that geometric subobjects form a Heyting subalgebra: the implication of two HML^+ -definable subfunctors is again computable by testing against a single canonical extension. This is an *irreducibly topos-theoretic* result: it requires both the presheaf Heyting implication formula (internal to the topos) and the canonical test extension construction. No purely process-algebraic proof is known.

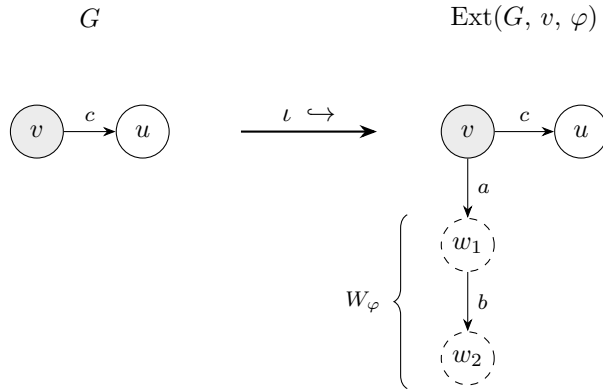


Figure 13: The free extension construction (Lemma 6.14). Given an LTS G with marked vertex v and a positive existential formula $\varphi = \langle a \rangle \langle b \rangle \top$, the extension $\text{Ext}(G, v, \varphi)$ adjoins a witness tree W_φ (dashed nodes) to G via the injection ι . Each diamond subformula contributes one fresh vertex (w_1 for $\langle a \rangle$, w_2 for $\langle b \rangle$), connected by the minimal edges required for satisfaction at $\iota(v)$. The original edges of G are preserved.

Corollary 6.17 (Subfunctor Heyting Adjunction). *For subfunctors S_1, S_2, T of the representable presheaf $\mathbf{y}(-)$ on C_{fp} , the Heyting implication satisfies the standard adjunction:*

$$S_1 \wedge T \leq S_2 \iff T \leq (S_1 \rightarrow_\Omega S_2),$$

where the partial order is pointwise inclusion.

Remark 6.18 (Explicit computations: four regimes). Over the alphabet $L = \{a, b\}$, the Geometric Closure Theorem yields four qualitatively distinct regimes for diamond-formula implications at depth ≤ 2 :

- (1) **Independent:** $\langle a \rangle \top \rightarrow \langle b \rangle \top = \langle b \rangle \top$. Extending by an a -successor adds no b -transitions; the implication reduces to ψ itself.
- (2) **Non-trivial residual:** $\langle b \rangle \top \rightarrow (\langle a \rangle \top \wedge \langle b \rangle \top) = \langle a \rangle \top$. The extension auto-satisfies $\langle b \rangle \top$ (the premise); the residual strips the freely provided part, leaving $\langle a \rangle \top$.
- (3) **Depth-increasing:** $\langle a \rangle \top \rightarrow \langle a \rangle \langle b \rangle \top = \langle a \rangle \langle b \rangle \top$. The shallow extension (single a -successor) cannot satisfy the deeper formula; the implication equals ψ .
- (4) **Entailment:** $\langle a \rangle \langle b \rangle \top \rightarrow \langle a \rangle \top = \top$. The stronger premise auto-provides the weaker conclusion; the implication is \top at every vertex of every LTS.

These four regimes exhaust the logical possibilities for diamond-formula implications at depth ≤ 2 and illustrate how the topos computes the “forced part,” the residual that remains after stripping away freely extensible structure. Each computation is a single evaluation of $\psi.\text{satisfies}(\text{Ext}(G, v, \varphi), \iota(v))$.

6.6. The trace Comparison Lemma. The trace topology on $\text{FinLTS}(L)$ admits a restriction to the full subcategory TraceLTS whose objects are linear chain LTS, one object $\text{traceLTS}(w)$ for each word $w \in L^*$. The density condition (every object in $\text{FinLTS}(L)$ is covered by trace objects) is proved constructively: for every $G : \text{FinLTS}(L)$, the sieve generated by morphisms factoring through trace objects is J_{trace} -covering (constructive). The general Comparison Lemma [25, C2.2.3] then yields:

$$\mathbf{Sh}(\text{FinLTS}(L), J_{\text{trace}}) \simeq \mathbf{Sh}(\text{TraceLTS}, J_{\text{trace}}|_{\text{TraceLTS}}).$$

Root-preserving homomorphisms between trace objects correspond to prefix embeddings: $\text{traceLTS}(w_1) \rightarrow \text{traceLTS}(w_2)$ exists iff $w_1 \leq_{\text{prefix}} w_2$, and when it exists it is unique. The restricted topology on TraceLTS is therefore the canonical topology on the prefix poset $(L^*, \leq_{\text{prefix}})$, and sheaves on a poset with the canonical topology are presheaves. Thus the trace topos is equivalent to $\text{PSh}(L^*, \leq_{\text{prefix}})$, precisely the Cattani–Winskel presheaf model for labeled event structures [13].

This identification connects 30 years of presheaf models for concurrency (Joyal–Nielsen–Winskel [26], Cattani–Winskel [13], Eberhart–Hirschowitz–Seiller [16]) to the topos-geometric framework of this paper: the abstract sheaf topos constructed from Grothendieck topologies on $\text{FinLTS}(L)$ restricts, via the Comparison Lemma, to the concrete presheaf category on a combinatorial poset. (Formalized: `comparison_lemma_synthesis`; the general Comparison Lemma, prefix-hom correspondence, and Cattani–Winskel connection are axiomatized.)

7. RELATED WORK

Preservation theorems. Van Benthem’s theorem [38] characterizes the bisimulation-invariant fragment of first-order logic as modal logic. Otto [32] gave an elementary proof avoiding compactness. Rosen [34] showed the characterization holds over finite structures. Rossman [35] proved the homomorphism-preservation theorem survives restriction to finite structures. Celani and Jansana [14] characterize the positive-bisimulation-invariant fragment of positive first-order logic as positive modal logic. Our Theorem 4.5 establishes the geometric (positive existential) case for pointed finite structures. Recent independent work by

Wałęga and Cuenca Grau [41] proves that over finite pointed Kripke models invariant under bounded unravellings, preservation under homomorphisms equals definability in existential positive modal logic, essentially the modal-theoretic substance of the geometric case under the standard translation. Their framework proceeds through the standard translation (modal logic to first-order), while our Theorem 4.5 works natively in geometric logic over classifying toposes; the two results are complementary.

Bisimulation and modal logic. Hennessy and Milner [19] introduced HML and proved the characterization theorem for image-finite systems: two states are bisimilar iff they satisfy the same HML formulas. Park [33] and Milner [31] developed the relational theory of bisimulation. Van Glabbeek [39] surveys the linear time–branching time spectrum for concrete sequential processes. Bisping [10, 9] recasts the spectrum as an energy-game hierarchy over 13 equivalences (replacing completed trace, completed simulation, and possible-worlds with impossible futures, revivals, and enabledness); §5.1 lifts this hierarchy to nuclei on Lindenbaum algebras.

Categorical and coalgebraic approaches. Joyal, Nielsen, and Winskel [26] characterized bisimulation via open maps in presheaf categories, a different setting from ours (the presheaf topos is the ambient category, not the classifying topos of a per-system theory). Abramsky [1] showed that in a domain-theoretic setting, propositional geometric logic (the observable properties) characterizes bisimulation: two processes are bisimilar iff they satisfy the same observable geometric properties. Our work concerns first-order geometric logic over per-system theories, a technically different framework, but the conceptual relationship is precise. At the propositional level, geometric logic and bisimulation see the same thing; Abramsky’s result provides the baseline. At the first-order level, quantifier structure introduces identification constraints that bisimulation can break: universal variables in antecedents can be equated in consequents (Mechanism 1), existential variables can share targets across branches (Mechanism 2), and variables can be identified with their sources (Mechanism 3). Our three-mechanism taxonomy is thus a classification of exactly how first-order quantification exceeds the propositional case. Abramsky and Shah [2] introduced game comonads, and Abramsky and Reggio [3] axiomatized them via *arboreal categories*, deriving equi-resource preservation theorems [4]. Our energy-to-nucleus map is structurally parallel: they encode resource-bounded equivalences as comonadic adjunctions on a universal presheaf category; we encode them as nuclei on per-system Lindenbaum algebras (= Lawvere–Tierney topologies on classifying toposes). A deeper difference concerns truncation: arboreal coKleisli morphisms operate at level 0 (full function data), as do our observation-class topologies for J_{trace} and J_{bisim} . Simulation, genuinely (-1) -truncated, requires the quotient-theory construction (Remark 6.7), an obstruction the arboreal framework avoids by not distinguishing simulation from bisimulation. Arboreal categories currently cover ~ 4 of the 13 named equivalences [5]; our framework targets all 13. Bezhanishvili, de Groot, and Venema [8] study coalgebraic geometric logic. Ghilardi and Zawadowski [18] connect sheaves, games, and model completions. Eberhart, Hirschowitz, and Seiller [16] provide the closest precedent for using Grothendieck topologies to encode behavioral equivalences. Working in a presheaf category on a category of terms (interaction trees for the π -calculus), they construct a Grothendieck topology whose sheaf condition enforces bisimulation: two terms have isomorphic sheafifications iff they are bisimilar. Their construction directly obtains bisimulation, the finest process equivalence, from a single topology. Our approach stratifies the *entire* spectrum: multiple topologies J_E

on a fixed site, one per equivalence, with the topology lattice reflecting the spectrum ordering (Theorem 6.8). The technical difference is that Eberhart–Hirschowitz–Seiller vary the terms (interaction trees of varying depth) while keeping the topology fixed to bisimulation; we fix the site (f.p.LTS $_L$) and vary the topology across the full spectrum.

Topos theory. Caramello [12] develops the systematic use of classifying toposes as “bridges” between mathematical theories. Johnstone [25] provides the foundational reference for classifying toposes and the Comparison Lemma. Makkai and Reyes [29] established the connection between geometric theories and their syntactic categories.

Realizability and the effective topos. Hyland [22] constructed the effective topos, whose internal logic validates Church’s Thesis. Hyland, Johnstone, and Pitts [23] introduced triposes as a uniform framework encompassing both provability and realizability toposes. Van Oosten [37] provides a comprehensive account of realizability categories and their categorical properties. Longley [28] identified a fundamental obstruction: even PCAs computing the same first-order functions yield inequivalent realizability toposes, the higher-type analogue of our Second Separation. Bauer [7] developed synthetic computability theory inside the effective topos, deriving Rice’s theorem and the recursion theorem from axioms (Number Choice, Enumerability, Markov’s Principle) without reference to a specific machine model.

Precedent: Kihara’s LT topologies. The closest structural parallel is Kihara [27], who connects bilayer imperfect-information games for Turing reducibility to Lawvere–Tierney topologies on the effective topos Eff . Both constructions use order-reversing maps from game budgets to closure operators on a subobject classifier: Kihara sends Turing-degree budgets to LT topologies on Ω_{Eff} ; we send energy vectors to nuclei on finite Lindenbaum frames L_d . A key divergence is algebraic: Kihara achieves a bijection on an uncountable Ω with rich negation ($x \wedge \neg x \neq \perp$ for many x); we achieve an embedding into a finite, negation-collapsed lattice ($\neg x = \perp$ for all $x \neq \perp$) where non-Booleanness comes entirely from the Heyting implication. Both witness non-Booleanness through Grothendieck topologies, but via complementary algebraic mechanisms.

Graded monads and the process spectrum. Dorsch, Milius, and Schröder [15] showed that the full van Glabbeek spectrum arises from graded monads: a graded monad $(T_n)_{n \in \mathbb{N}}$ on Set parameterizes look-ahead depth, and a generic Hennessy–Milner theorem holds for each grading. Our Section 5.1 embeds this spectrum as a subtopos lattice via Caramello’s duality theorem, extending the coalgebraic perspective to topos-theoretic invariants. The energy-to-nucleus map of §5.1 makes the grading explicit: each energy vector \bar{e} induces a Lawvere–Tierney topology $j_{\bar{e}}$, turning the graded spectrum into a lattice of subtoposes.

Automata topoi. Hora [20, 21] constructs four topoi for regular languages using Caramello’s bridge technique, the closest methodological parallel. Structurally, automata have no branching, so acceptance is inherently (-1) -truncated and all four topologies arise from observation classes with no quotient-theory detour. Our transition-system setting, where path multiplicity matters (tree homs vs tree-hom existence), introduces the truncation-level split that non-trivially stratifies the spectrum.

Database theory. Yannakakis [42] introduced acyclic hypergraphs for conjunctive queries. The tree-shaped fragment characterizing the bisimulation-invariant geometric formulas corresponds to acyclic conjunctive queries over the binary step relation.

8. CONCLUSION

This paper develops the foundations of a unification between topos theory and process algebra, in which the question “when should two computational systems be considered equivalent?” receives a single structural answer: two finitely presentable systems are equivalent, relative to a choice of observations, when their sheafified Yoneda images become isomorphic in the subtopos determined by that choice. The van Glabbeek spectrum, traditionally a hierarchy of behavioral equivalences, each justified by its own operational or logical intuition, is revealed to be a finite sub-poset of the coframe of subtoposes of a classifying topos, and the passage from one equivalence to another is localization.

The evidence comes from three directions. The *geometric* direction constructs explicit Grothendieck topologies J_{trace} , J_{sim} , and J_{bisim} on the site of finitely presentable labeled transition systems, with a strict chain $J_{\text{bisim}} \subsetneq J_{\text{sim}} \subsetneq J_{\text{trace}}$ extended to all 13 named equivalences by the Energy–LT Bridge (Theorem 6.10). The trace and bisimulation topologies are explicitly defined via observation classes; the simulation topology is obtained via Caramello’s quotient-theory duality [12], and a constructive counterexample (Theorem 6.5) proves this indirect route structurally necessary; a truncation-level mismatch between the propositional content of simulation and the set-level data carried by sieves. The *algebraic* direction closes the 13 named equivalences under lattice operations to obtain the 30-element spectrum lattice L_{30} (notation introduced here for the lattice closure of the van Glabbeek spectrum under meets and joins) with its bi-Heyting structure, including the identity $S \rightarrow F = \text{IF}$, 17 unnamed hybrids, and direct indecomposability, all proved with zero custom axioms. The *logical* direction identifies the boundary between topos-level and process-level expressiveness: the Geometric van Benthem Theorem characterizes diamond-only Hennessy–Milner logic as the bisimulation-invariant fragment of geometric logic, while the Geometric Closure Theorem reduces presheaf Heyting implications to testing at a single free extension, a reduction specific to the combinatorial structure of the LTS site, where the canonical one-step extension serves as a generic witness in place of Kripke–Joyal’s universal quantification over all extensions.

The conceptual payoff is that the classifying topos provides a *uniform* framework for computational symmetries. Each behavioral equivalence is a Grothendieck topology; the space of all such equivalences is a coframe; and the algebraic operations of this coframe, meets, Heyting implications, co-Heyting subtractions, produce structure that process algebra cannot access internally. The 17 unnamed elements of L_{30} are the most concrete manifestation: they are process equivalences discovered through the coframe structure, invisible to any single energy budget, corresponding to geometric axioms (determinism, image-finiteness, mixed constraints) that cross-cut the classical spectrum. The embedding $\nu: \mathcal{V} \hookrightarrow \text{Sub}(\text{Set}[\mathbb{T}_{\text{LTS}}])^{\text{op}}$ is an order-embedding of a 13-element poset into an infinite coframe; whether it extends to a *sublattice* embedding of L_{30} , with meets and joins agreeing with the ambient coframe operations, remains the central structural conjecture.

This framework is not specific to the van Glabbeek spectrum. Any family of geometric theories whose models are computational systems, and any family of quotient axioms corresponding to observational abstractions, produces a lattice of subtoposes in which the same questions can be asked: what are the lattice operations? What unnamed equivalences

arise? Is the embedding a sublattice? The present paper answers these questions for labeled transition systems and the energy-game hierarchy; the techniques, Lindenbaum algebras, nucleus maps, observation-class topologies, Caramello’s duality [12], are general. Extensions to other computational models (automata, event structures, Petri nets) whose equivalences are expressible as geometric quotients are natural next steps; models involving quantitative reasoning (probabilistic or quantum systems) would require enrichment of the logical framework beyond geometric sequents.

The simulation topology is established abstractly via Caramello’s duality; the recent generation formulas of Caramello–Lafforgue [11] offer a path to explicit covering sieves, which would eliminate the axioms for J_{sim} . Whether the full 30-element closure embeds as a *sublattice* of the subtopos coframe, meets and joins agreeing, remains the central structural question; a positive answer would give L_{30} a coordinatization-free characterization, resolving the dependence on Bisping’s energy-game parameterization noted in Remark 5.3. More broadly, whether every Grothendieck topology between J_{bisim} and J_{trace} arises from an observation class would yield a bijective correspondence between behavioral equivalences and subtoposes, a structural embedding of the two traditions this paper connects.

Formalization. A Lean 4 formalization using Mathlib [30] accompanies this paper, comprising 118 files in the `RuleSys` library. The headline results, HML bisimulation invariance (Theorem 4.2), the Geometric Closure Theorem 6.16, the L_{30} bi-Heyting structure (Theorems 5.9–5.11), both Grothendieck topologies J_{trace} and J_{bisim} (Theorem 6.3), the naive simulation instability (Theorem 6.5), characteristic formulas (Lemma 4.13), and the depth 0–2 van Benthem instances (Theorems 4.7–4.10), are proved with zero custom axioms. The axiomatized components mark the interface with published results, Caramello’s quotient-theory duality [12], van Glabbeek’s logical characterization theorems [39], and Bisping’s energy-game framework [9], whose Lean formalization awaits the development of Mathlib’s topos-theoretic infrastructure. The full codebase is available at `K-NANOG/spectrum-topos`.

REFERENCES

- [1] S. Abramsky. Domain theory in logical form. *Annals of Pure and Applied Logic*, 51, 1991.
- [2] S. Abramsky and N. Shah. Relating structure and power: comonadic semantics for computational resources. *Journal of Logic and Computation*, 31(6), 2021.
- [3] S. Abramsky and L. Reggio. Arboreal categories: an axiomatic theory of resources. *Logical Methods in Computer Science*, 19(3:14), 2023.
- [4] S. Abramsky and L. Reggio. Arboreal categories and equi-resource homomorphism preservation theorems. *Annals of Pure and Applied Logic*, 175(6):103423, 2024.
- [5] S. Abramsky, Y. Montacute, and N. Shah. Linear arboreal categories. *arXiv:2301.10088*, 2023.
- [6] L. Aceto, A. Achilleos, A. Chalki, and A. Ingólfssdóttir. The complexity of deciding characteristic formulae modulo nested simulation. *arXiv:2505.22277*, 2025.
- [7] A. Bauer. First steps in synthetic computability theory. *Electronic Notes in Theoretical Computer Science*, 155, 2006.
- [8] N. Bezhanishvili, J. de Groot, and Y. Venema. Coalgebraic geometric logic: basic theory. *Logical Methods in Computer Science*, 18(4:10), 2022.
- [9] B. Bisping. Process equivalence problems as energy games. In *Proc. CAV 2023*, LNCS **13964**, Springer, 2023.
- [10] B. Bisping. *Generalized Equivalence Checking of Concurrent Programs*. PhD thesis, TU Berlin, 2025.
- [11] O. Caramello and L. Lafforgue. Generation of Grothendieck topologies, provability and operations on subtoposes. *arXiv:2508.21134*, 2025.
- [12] O. Caramello. *Theories, Sites, Toposes*. Oxford University Press, 2018.

- [13] G. L. Cattani and G. Winskel. Profunctors, open maps and bisimulation. *Mathematical Structures in Computer Science*, 15(3), 2005.
- [14] S. Celani and R. Jansana. Priestley duality, a Sahlqvist theorem and a Goldblatt–Thomason theorem for positive modal logic. *Logic Journal of the IGPL*, 7(6), 1999.
- [15] U. Dorsch, S. Milius, and L. Schröder. Graded monads and graded logics for the linear time–branching time spectrum. In *Proc. CONCUR 2019*, LIPIcs **140**, 2019.
- [16] C. Eberhart, T. Hirschowitz, and T. Seiller. An intensionally fully-abstract sheaf model for π (expanded version). *Logical Methods in Computer Science*, 13(4:9), 2017.
- [17] N. Funayama and T. Nakayama. On the distributivity of a lattice of lattice-congruences. *Proc. Imp. Acad.*, 18(9), 1942.
- [18] S. Ghilardi and M. Zawadowski. *Sheaves, Games, and Model Completions*. Kluwer Academic Publishers, 2002.
- [19] M. Hennessy and R. Milner. Algebraic laws for nondeterminism and concurrency. *J. ACM*, 32(1), 1985.
- [20] R. Hora. Topoi of automata I: Four topoi of automata and regular languages. *arXiv:2411.06358*, 2024.
- [21] R. Hora. Topoi of automata. Presented at CT2025, Brno, 2025.
- [22] J. M. E. Hyland. The effective topos. In *The L.E.J. Brouwer Centenary Symposium*, Studies in Logic and the Foundations of Mathematics **110**, North-Holland, 1982.
- [23] J. M. E. Hyland, P. T. Johnstone, and A. M. Pitts. Tripos theory. *Mathematical Proceedings of the Cambridge Philosophical Society*, 88(2), 1980.
- [24] P. T. Johnstone. *Stone Spaces*. Cambridge University Press, 1982.
- [25] P. T. Johnstone. *Sketches of an Elephant: A Topos Theory Compendium*. Oxford University Press, 2002.
- [26] A. Joyal, M. Nielsen, and G. Winskel. Bisimulation from open maps. *Information and Computation*, 127(2), 1996.
- [27] T. Kihara. Lawvere–Tierney topologies for computability theorists. *Trans. Amer. Math. Soc. Ser. B*, 10, 2023.
- [28] J. Longley. Notions of computability at higher types I. In *Logic Colloquium 2000*, Lecture Notes in Logic **19**, ASL, 2005.
- [29] M. Makkai and G. E. Reyes. *First Order Categorical Logic*. Springer, 1977.
- [30] The mathlib Community. The Lean mathematical library. In *Proc. CPP 2020*, ACM, 2020.
- [31] R. Milner. *Communication and Concurrency*. Prentice Hall, 1989.
- [32] M. Otto. Elementary proof of the van Benthem–Rosen characterisation theorem. Technical Report 2342, TU Darmstadt, 2004.
- [33] D. Park. Concurrency and automata on infinite sequences. In *Theoretical Computer Science*, LNCS **104**, Springer, 1981.
- [34] E. Rosen. Modal logic over finite structures. *J. Logic, Language and Information*, 6(4), 1997.
- [35] B. Rossman. Homomorphism preservation theorems. *J. ACM*, 55(3), 2008.
- [36] J. J. M. M. Rutten. Universal coalgebra: a theory of systems. *Theoretical Computer Science*, 249(1), 2000.
- [37] J. van Oosten. *Realizability: An Introduction to its Categorical Side*. Studies in Logic and the Foundations of Mathematics **152**, Elsevier, 2008.
- [38] J. van Benthem. Modal correspondence theory. PhD thesis, University of Amsterdam, 1976.
- [39] R. van Glabbeek. The linear time–branching time spectrum I. In *Handbook of Process Algebra*, Elsevier, 2001.
- [40] R. van Glabbeek. The linear time–branching time spectrum II. In *Proc. CONCUR 1993*, LNCS **715**, Springer, 1993.
- [41] P. A. Wałęga and B. Cuenca Grau. Preservation theorems for unravelling-invariant classes: a uniform approach for modal logics and graph neural networks. *arXiv:2602.01856*, 2026.
- [42] M. Yannakakis. Algorithms for acyclic database schemes. In *Proc. VLDB*, 1981.